11-1-2010

Distribution of Capillary Transit Times in Isolated Lungs of Oxygen-Tolerant Rats

Madhavi Ramakrishna
Marquette University

Zhuohui Gan
Marquette University

Anne V. Clough
Marquette University, anne.clough@marquette.edu

Robert C. Molthen
Marquette University, robert.molthen@marquette.edu

David L. Roerig
Medical College of Wisconsin

See next page for additional authors

Accepted version. *Annals of Biomedical Engineering*, Vol. 38, No. 11 (November 2010): 3449-3465.

Distribution of Capillary Transit Times in Isolated Lungs of Oxygen-Tolerant rats

Madhavi Ramakrishna
Department of Biomedical Engineering, Marquette University
Milwaukee, WI

Zhuohui Gan
Department of Biomedical Engineering, Marquette University
Milwaukee, WI

Anne V. Clough
Department of Biomedical Engineering, Marquette University
Milwaukee, WI
Department of Mathematics, Statistics and Computer Science, Marquette University
Milwaukee, WI
Division of Pulmonary and Critical Care Medicine, Medical College of Wisconsin
Milwaukee, WI

Robert C. Molthen
Department of Biomedical Engineering, Marquette University
Milwaukee, WI
Division of Pulmonary and Critical Care Medicine, Medical College of Wisconsin

Annals of Biomedical Engineering, Vol. 38, No. 11 (November 2010): pg. 3449-3465. DOI.

Research Service 151, Zablocki V.A. Medical Center
Milwaukee, WI

David L. Roerig
Department of Anesthesiology, Medical College of Wisconsin
Milwaukee, WI
Department of Pharmacology/Toxicology, Medical College of Wisconsin
Milwaukee, WI
Research Service 151, Zablocki V.A. Medical Center
Milwaukee, WI

Said H. Audi
Department of Biomedical Engineering, Marquette University
Milwaukee, WI
Division of Pulmonary and Critical Care Medicine, Medical College of Wisconsin
Research Service 151, Zablocki V.A. Medical Center
Milwaukee, WI

Abstract:

Rats pre-exposed to 85% O_2 for 5–7 days tolerate the otherwise lethal effects of 100% O_2. The objective was to evaluate the effect of rat exposure to 85% O_2 for 7 days on lung capillary mean transit time ($\bar{t}_c$) and distribution of capillary transit times ($h_c(t)$). This information is important for subsequent evaluation of the effect of this hyperoxia model on the redox metabolic functions of the pulmonary capillary endothelium. The venous concentration vs. time outflow curves of fluorescein isothiocyanate labeled dextran (FITC-dex), an intravascular indicator, and coenzyme Q_1 hydroquinone (CoQ_1H_2), a compound which rapidly equilibrates between blood and tissue on passage through the pulmonary circulation, were measured following their bolus injection into the pulmonary artery of isolated perfused lungs from rats exposed to room air (normoxic) or 85% O_2 for 7 days (hyperoxic). The moments (mean transit time and variance) of the measured FITC-dex and CoQ_1H_2 outflow curves were determined for each lung, and were then used in a mathematical model [Audi *et al. J. Appl. Physiol*. 77: 332–351, 1994] to

Annals of Biomedical Engineering, Vol. 38, No. 11 (November 2010): pg. 3449-3465. DOI.

estimate $\bar{t}_c$ and the relative dispersion (RD_c) of $h_c(t)$. Data analysis reveals that exposure to hyperoxia decreases lung $\bar{t}_c$ by 42% and increases RD_c, a measure $h_c(t)$ heterogeneity, by 40%.

Keywords: Perfusion heterogeneity, Hyperoxia, Coenzyme Q_1, Multiple indicator dilution, Flow-limited indicators, Angiotensin converting enzyme.

INTRODUCTION

The most common initial treatment of hypoxemia in adults with significant lung (e.g., acute respiratory distress syndrome, pneumonia) or heart disease and premature infants with respiratory distress syndrome is oxygen (O_2) therapy (normobaric hyperoxia).[14,38,49] However, exposure to high O_2 concentrations (>50%) for prolonged periods is toxic, particularly to the lungs.[15,23,27,28,55] Although the mechanisms leading up to pulmonary hyperoxic injury are not fully understood, it is widely believed that the deleterious effects of high O_2 are the result of increased formation of reactive oxygen species (ROS), which at high concentrations cause various cytotoxic effects.[26,29,30,34,37,40,54] Presently, there are no known effective ways to mitigate the toxic side effects of O_2 therapy.

The rat model of hyperoxic lung injury mimics several aspects of lung O_2 toxicity observed clinically. When adult rats are exposed to 100% O_2 environment, they die within 60–72 h of lung injury.[21,22] However, if adult rats are exposed to sublethal 85% O_2 environment for 5–7 days, they acquire tolerance to 100% O_2 in that if transferred to 100% O_2 environment they survive for prolonged periods.[3,21,28,52] This tolerance is not observed in other rodent species, but a similar tolerance occurs in humans.[19,23] Elucidating the factors that contribute to this tolerance has the potential to further our understanding of the mechanisms involved in lung O_2 toxicity and for identifying potential therapeutic targets for mitigating the toxic side effects of O_2 therapy.[3,21,23,28,52]

Studies by Crapo *et al*. provide a detailed description of histologic and morphometric changes in lungs of rats exposed to 85% O_2 for up to 14 days.[21,22] For the first 72 h of exposure, signs of histologic and/or morphometric changes are undetectable.[21,22] By 5 days, there is ~30% loss in capillary endothelial cells and cell surface, infiltration of phagocytic leukocytes and other cell types, and an

increase in the thickness of air–blood barrier. By 7 days, inflammation is still evident and the lungs have lost half of the capillary endothelial cells, but pleural effusion and respiratory function impairment have substantially subsided. Capillary endothelial cells that survive 7 days at 85% O_2 experience significant morphometric changes including hypertrophy (76%), with no further loss of these hypertrophied endothelial cells occurring between 7 and 14 days of exposure.[21,22] These studies reveal that the pulmonary capillary endothelium is a primary target of lung O_2 toxicity, and suggest that biochemical changes in hypertrophied capillary endothelial cells are potentially important to the acquired tolerance to 100% O_2.

Previous studies have demonstrated hyperoxia-induced changes in the activities of pro- and anti-oxidant redox enzymes, predominantly in lung tissue homogenates, and have suggested that redox enzymes, among other factors, play a role in rat tolerance to 100% O_2 induced by pre-exposure to 85% O_2 for 5–7 days.[3,21,23,28,35,39,52] However, the results of these *in vitro* studies do not necessarily predict hyperoxia-induced changes in the activities of redox enzymes in an intact lung.[3,5] This is because potential changes in key aspects of the enzyme environment in an intact lung that may influence redox enzyme kinetics (e.g., competing redox enzymes, tissue permeation of electron acceptors, availability of electron donors, tissue perfusion) are not preserved. Thus, a change in the activity of a redox enzyme measured in lung tissue homogenate may not be representative of the change in its activity in the intact lung.[3,5] Furthermore, depending on the effect of hyperoxia on the activities of redox enzymes in various lung cell types, this *in vitro* approach may overestimate or underestimate hyperoxia-induced changes in the activities of redox enzymes in pulmonary capillary endothelial cells that survived exposure to 85% O_2 for 7 days.[3,21,22] This issue is especially important for lungs of rats exposed to 85% O_2 for 7 days since the wet and dry weights of these lungs almost double mostly due to the large increase in the number of interstitial cells (~250%), while the number of capillary endothelial cells is half that of normoxic lungs.[21,22] As a result, the cellular composition of these lungs changes significantly: the number of capillary endothelial cells as a percent of the total number of lungs cells decreases form ~45% (normoxic lungs) to ~15%, and the number of interstitial cells increases from ~29% (normoxic lungs) to ~54%.[21,22] However, there are limited data on the

Annals of Biomedical Engineering, Vol. 38, No. 11 (November 2010): pg. 3449-3465. DOI.

activities of redox enzymes in the intact lungs, in part because of the complexity of the intact lung.[2-4,9,10,16]

Multiple indicator dilution (MID) methods have been an important research tool for evaluating capillary endothelial metabolic functions within a functioning organ.[2,5,13,25,50,57] These methods involve the bolus injection or finite pulse infusion of two or more indicators into the organ's arterial inlet, followed by measurement of their concentrations in the venous effluent as a function of time. The injected indicators usually include an intravascular indicator (i.e., confined to the vasculature of the organ) plus a test indicator that is a substrate or ligand for the metabolic function(s) of interest within the organ. The interactions of the test indicator with these metabolic function(s) on passage though the organ result in characteristic differences between the intravascular and test indicator venous effluent concentration vs. time curves.

The information content of data resulting from MID methods can be complex. In addition to the targeted tissue metabolic processes (e.g., redox enzymes), other factors can influence the amount of test indicator that is removed and/or modified on passage through the organ. These include the subject of this investigation, namely, organ capillary perfusion kinematics (e.g., capillary mean transit time ($\bar{t}_c$) and distribution of capillary transit times ($h_c(t)$)).[2,3,7] The longer the capillary transit time, the more time available for test indicators to interact with targeted tissue metabolic processes. Furthermore, it can be shown mathematically that, all else being equal, the rate of test indicator interaction with tissue components is inversely proportional to the heterogeneity of the capillary transit time distribution.[2,7,31] Thus, a change in measured indicator dilution data could be a result of a change in the activity of metabolic functions (e.g., redox enzymes), a change in organ perfusion kinematics, or a combination of both. Therefore, proper interpretation of MID data in terms of the kinetics of test indicator interactions with tissue metabolic processes can be confounded without an independent determination of the capillary transit time distribution and its mean.[2,7] This is especially important for lungs of rats exposed to 85% O_2 for 7 days which experience ~50% loss of capillary volume and endothelial surface area.[21,22] To the best of our knowledge, there is no information regarding the effect of rat exposure to this hyperoxia model on $h_c(t)$ in the intact lungs.

Annals of Biomedical Engineering, Vol. 38, No. 11 (November 2010): pg. 3449-3465. DOI.

Previously we developed an MID method for estimating capillary mean transit time and the distribution of capillary transit times in isolated perfused lungs and applied it to isolated perfused dog lung lobes, rabbit lung, and rat lung.[2,6,8] The method involves the arterial bolus injection of an intravascular indicator and a test indicator that rapidly equilibrates (i.e., "flow-limited") between blood and tissue on passage through the organ's capillary or microvascular region, and the simultaneous measurement of their concentrations in the venous effluent as function of time.[6,8,32] The method is based on the concept that comparison of the dispersion of an intravascular indicator and a flow-limited indicator which behaves the same way as the intravascular indicator within the conducting vessels, but can rapidly equilibrate between blood and tissue within the pulmonary capillaries, will provide information necessary to determine the moments of $h_c(t)$, i.e., mean transit time (first moment; $\bar{t}_c$) and variance (second central moment; σ2c).

Recently, we demonstrated that the reduced form (CoQ_1H_2) of coenzyme Q_1 (CoQ_1; 2,3-dimethoxy-5-methyl-6-[3-methyl-2-butenyl]-1,4-benzoquinone), redox active quinone, rapidly equilibrates between the perfusate and the tissue on passage through isolated perfused rat lungs.[9] Thus, the objective of this study was to utilize the above MID method, with CoQ_1H_2 as the flow-limited test indicator and fluorescein isothiocyanate labeled dextran (FITC-dex) as the intravascular indicator, to determine the effect of rat exposure to 85% O_2 for 7 days (hyperoxic rats) on $\bar{t}_c$ and $h_c(t)$.

EXPERIMENTAL METHODS

Materials

CoQ_1 and other chemicals were purchased from Sigma (St. Louis, MO), unless noted otherwise. CoQ_1H_2 was prepared by reduction of CoQ_1 with potassium borohydride (KBH_4) as previously described.[3] Bovine serum albumin (BSA) was purchased from Serologicals Inc. (Gaithersburg, MD).

Annals of Biomedical Engineering, Vol. 38, No. 11 (November 2010): pg. 3449-3465. DOI.

Animals

For normoxic lung studies, male Sprague–Dawley rats (~300 g; Charles River) were exposed to room air. For the hyperoxic lung studies, age-matched rats were housed in a Plexiglas chamber (13*W* × 23*L* × 12*H* in.) maintained at ~85% O_2, balance N_2 for 7 days with free access to food and water as previously described.[3] The total gas flow was ~3.5 L/min, and the chamber CO_2 was maintained at <0.5%. The temperature within the chamber was maintained at ~21 °C using a custom built cooling system. The chamber was opened every other day for ~15 min to clean the cage, weigh the animals, and replace food, water, and CO_2 absorbent. The protocol was approved by the Institutional Animal Care and Use Committees of the Zablocki Veterans Affairs Medical Center and Marquette University (Milwaukee, WI). A total of 12 normoxic rats and 8 hyperoxic rats were studied.

Isolated Perfused Rat Lung

The isolated perfused rat lung preparation has been previously described.[3,9] Briefly, each rat was anesthetized with pentobarbital sodium (40 mg/kg body wt. i.p.). The trachea was clamped, the chest opened and heparin (0.7 IU/g body wt.) was injected into the right ventricle, and a blood sample was taken for determining blood hematocrit. The pulmonary artery and the trachea were cannulated, and the pulmonary venous outflow was accessed via a cannula in the left atrium. For the pressure-flow experiments, the heart was excised and the pulmonary vein was open to atmosphere. The lung was removed from the chest and attached to a ventilation–perfusion system. The control perfusate contained in mM 4.7 KCl, 2.51 $CaCl_2$, 1.19 $MgSO_4$, 2.5 KH_2PO_4, 118 NaCl, 25 $NaHCO_3$, 5.5 glucose, and 5% BSA.[2,3,9] The single pass perfusion system was primed (Master-flex roller pump) with the control perfusate maintained at 37 °C and equilibrated with 15% O_2, 6% CO_2, balance N_2 resulting in perfusate P_{O2}, P_{CO2} and pH of ~105 Torr, 40 Torr, and 7.4, respectively. Initially, control perfusate was pumped through the lung until the lung was evenly blanched and the venous effluent was clear of red blood cells, as determined by visual inspection. The lung was ventilated (40 breaths/min) with end-inspiratory and end-expiratory pressures of 6 and 3 mmHg, respectively, with the above gas mixture. The pulmonary arterial pressure was referenced to atmospheric pressure at

the level of the left atrium and monitored continuously during the course of the experiments. The venous outflow was referenced to atmospheric pressure. At the end of each experiment, the lung was weighed, and then dried (60 °C) to a constant weight for the determination of lung dry weight.

Multiple Indicator Dilution Experiments

An injection loop was included in the arterial line of the ventilation–perfusion system to allow the introduction of a ~0.1 mL bolus into the arterial inflow without altering the flow or perfusion pressure.[2,3,9] The injection loop consisted of a Y-tube on the outflow side of the pump, which allowed perfusate to flow through either side of two parallel segments of tubing, each containing ~0.8 mL volume. A double solenoid pinch valve permitted flow through only one segment at any time. Thus, a bolus injection was made by injecting the indicator into the stagnant segment (while perfusate was flowing through the other segment into the lung) and then activating the solenoid pinch valve, so that the flow was directed through the indicator-containing segment. This allowed for the bolus to be introduced without changing pressure or flow. At the same time the solenoid pinched value was activated, the lung effluent was simultaneously diverted into the sampling tubes of a sample collector.

Each lung was perfused with control perfusate containing 2 mM potassium cyanide (KCN) for 5 min at perfusate flow of 10 mL/min to inhibit mitochondrial complex III, which is the dominant site of CoQ_1H_2 oxidation on passage through the rat lung.[9] The respirator was then stopped at end expiration and a 0.1 mL bolus of control perfusate containing 2 mM KCN and either 35 μM FITC-dex or 1200 μM CoQ_1H_2 was injected into the pulmonary arterial inflow tubing. Simultaneous to each bolus injection, the venous effluent was diverted into a modified Gilson Escargot fraction collector for continuous collection of lung effluent.[2,3,9] For the FITC-dex bolus injection, 60 samples (0.15 mL each) were collected at a sampling interval of 0.9 s at a perfusate flow of 10 mL/min. For the CoQ_1H_2 injection, 60 samples (0.3 mL each) were collected at a sampling interval of 1.8 s at a flow of 10 mL/min.

Previously, we derived the following relationship between the perfusate albumin (BSA) concentration and the extravascular mean

Annals of Biomedical Engineering, Vol. 38, No. 11 (November 2010): pg. 3449-3465. DOI.

residence time ($\bar{t}_e$) of a flow-limited indicator on passage through the pulmonary circulation[6,8]

$$\bar{t}_e = \frac{MQ_t}{F\left(1 + \frac{[BSA]}{K}\right)}, \quad (1)$$

where M is the tissue-to-plasma partition coefficient of the flow-limited indicator, K is the indicator–BSA binding equilibrium dissociation constant, F is the perfusate flow, Q_t is the extravascular tissue volume accessible by the flow-limited indicator from the vascular region, and [BSA] is the perfusate BSA concentration. [6,8] Equation (1) suggests that the value of $\bar{t}_e$ for CoQ_1H_2 on passage through the lung can be manipulated by altering the perfusate BSA concentration. Hence, bolus injections of CoQ_1H_2 at different perfusate BSA concentrations can provide data equivalent to that which would be obtained with bolus injections of different flow-limited indicators having different $\bar{t}_e$ values.[6] Thus, to evaluate the sensitivity of the estimated $\bar{t}_c$ and $h_c(t)$ to the value of $\bar{t}_e$ we examined the effect of perfusate BSA concentration on CoQ_1H_2 outflow curve following its arterial bolus injection. After the first two bolus injections with perfusate containing 5% BSA (control perfusate), the perfusate reservoir was refilled with an appropriate volume of fresh perfusate containing 3% BSA and 2 mM KCN. This was followed by another 0.1-mL bolus injection of 3% BSA perfusate containing KCN and CoQ_1H_2, and sampling of the venous effluent as described above. Subsequently, another CoQ_1H_2 bolus injection was carried out with the perfusate BSA concentration at 10%

An index of perfused lung capillary surface area was estimated as previously described.[3,9] Briefly, a 150 μM 20-s pulse infusion of the angiotensin converting enzyme (ACE) substrate *N*-[3-(2-Furyl)acryloyl]-Phe-Gly-Gly (FAPGG) was introduced into the lung using the control perfusate at a flow of 30 mL/min. Two venous effluent samples (~1.0 mL each) were collected between 15 and 20 s after the start of the infusion.[3,9] The permeability–surface area product (PS, mL/min) for FAPGG, which is a measure of lung ACE activity, was

determined using Eq. (2) from the FAPGG concentrations measured in the venous effluent samples as previously described[3,9]:

$$PS = -F \ln(1-E) \qquad (2)$$

where ***E* = steady state extraction ratio =** $1 - \frac{[FAPGG]_o}{FAPGG_i}$; $[FAPGG]_i$ is the infused arterial FAPGG concentration; $[FAPGG]_o$ is the steady state venous effluent FAPGG concentration calculated as the average [FAPGG] in the collected venous effluent samples, and *F* is the perfusate flow. The PS product is considered here to be an index of perfused capillary surface area.[3,9] For all normoxic and hyperoxic lungs studied, the FAPGG pulse infusion was carried out at the beginning and at the end of the CoQ_1H_2 and FITC-dex bolus injection protocol described above to evaluate the stability of the lung over the time course of the experiments.

At the end of the above bolus injections and FAPGG pulse infusion protocol the lung was removed from the perfusion system, the arterial and venous cannulae were connected, and the reservoir was refilled with control perfusate. An FITC-dex (35 μM) bolus injection at a perfusate flow of 10 mL/min was then carried out. Thirty samples (0.15 mL each) were collected at a sampling interval of 0.9 s. These data were used to determine the tubing transit time of the perfusion system and the bolus dispersion outside the lung.

The concentrations of CoQ_1H_2 in the venous effluent samples were determined as previously described.[2,3,9] Briefly, the venous effluent samples were first centrifuged (1 min at 5,600×*g*). For each sample, 100 μL of supernatant was then added to a centrifuge tube containing 10 μL potassium ferricyanide (12.1 mM in deionized H_2O) to oxidize CoQ_1H_2 to CoQ_1. Cold, absolute ethanol (~0.6 mL) was added, and the tube was mixed on a vortex mixer followed by centrifugation at 9,300×*g* for 5 min at 4 °C. A perfusate sample that had passed through the lungs but contained no CoQ_1H_2 was treated in the same manner and used as the blank for absorbance measurements. The concentration of CoQ_1 (μM) in each perfusate sample, which is equal to sample CoQ_1H_2 concentration prior to the addition of potassium ferricyanide, was calculated from the absorbance of the fully oxidized supernatant in the tube at 275 nm (Beckman DU 7400

spectrophotometer) using a molar extinction coefficient of 14.30 mM^{-1} cm^{-1} for CoQ_1.

The concentration of FITC-dex in each of the venous effluent samples was determined from the sample absorbance at 495 nm using a molar extinction coefficient of 93.5 mM^{-1} cm^{-1}.[2,3,9]

The calculated recoveries for FITC-dex and CoQ_1H_2 in the venous effluent samples were 93 ± 6 (SE) and 101 ± 1% for normoxic lungs, and 106 ± 5 and 109 ± 3% for hyperoxic lungs, respectively.

Pressure-Flow Measurements

To evaluate the effect of rat exposure to hyperoxia on the distensibility and vasodilatory properties of the pulmonary vascular bed, we carried out the following pressure-flow experiments on a group of normoxic and hyperoxic lungs. The lung was perfused with control perfusate at 10 mL/min and ventilated for several minutes, after which ventilation was halted and the lung was held at an airway pressure of 6 mmHg. The arterial pressure was then measured at flows of 35, 30, 25, 20, 15, 10, and 5 mL/min. The pump was then stopped and after ~15 s, long enough for the arterial pressure to reach equilibrium, a critical closing pressure (arterial pressure at zero flow) was recorded. Ventilation was then resumed, and the lung was perfused with control perfusate containing the vasodilator papaverine hydrochloride (0.6 mg/mL) for 4 min, after which ventilation was again halted and the above pressure-flow protocol was repeated.[51]

Statistical Evaluation of Data

Statistical comparisons were carried out using paired *t*-test, unpaired *t*-test, or ANOVA followed by Dunnett's test, with $p < 0.05$ as the criterion for statistical significance.

EXPERIMENTAL RESULTS

Over the 7-day hyperoxic exposure period, rats lost ~10% of their pre-exposure body weights. During the first 48 h of exposure to hyperoxia, rats maintained their body weights, while between days 2

and 6, body weights decreased steadily. By day 7, the rats stopped losing body weight.

Exposure to hyperoxia increased lung wet and dry weights by ~100%, with no significant effect on wet/dry weight ratios as compared to normoxic lungs (Table 1). The lung wet weights of hyperoxic rats measured in this study (2.4 ± 0.21 (SE) g) are consistent with those reported by Crapo *et al*. (2.29 ± 0.44 (SD) g for ~290 g rats) for the same exposure period.[21] The lack of a significant difference in wet/dry weight ratios between normoxic and hyperoxic lungs (Table 1) is consistent with the hyperoxia-induced increase in lung wet weight being due to increase in lung cell mass rather than edema as shown by Crapo *et al*.[21,22]

	Body wt. (g)	Wet wt. (g)	Dry wt. (g)	Wet/dry wt.	Aortic blood hematocrit
Normoxic	302 ± 9	1.20 ± 0.07	0.22 ± 0.01	5.76 ± 0.16	42.5 ± 0.7
Hyperoxic	284 ± 5	2.40 ± 0.21*	0.40 ± 0.03*	5.87 ± 0.09	49.1 ± 0.5

TABLE 1 Rat body weights, lung wet weights, lung dry weights, lung wet/dry weight ratios, and aortic blood hematocrit.

Values are mean ± SE. n = 12 (normoxic) and n = 8 (hyperoxic) for body wt., lung dry wt. and blood hematocrit. For lung wt. and wet/dry wt., n = 9 and 5 for normoxic and hyperoxic lungs, respectively.

*Significantly different between normoxic and hyperoxic lungs (t-test; $p < 0.05$).

Exposure to hyperoxia increased aortic blood hematocrit by ~15% (Table 1). This increase, which was also observed by Crapo *et al*. for the same exposure period, could be due to dehydration as suggested by Crapo *et al*.[21,22]

Exposure to hyperoxia decreased PS (mL/min), which is a measure of lung ACE activity and an index of perfused capillary surface area, on average by 56% (Table 2). The PS values obtained from FAPGG pulse infusions carried out at the beginning and at the end of the bolus injection protocol were not significantly different (Table 2), indicating that perfusion and/or multiple bolus injections of CoQ_1H_2

Annals of Biomedical Engineering, Vol. 38, No. 11 (November 2010): pg. 3449-3465. DOI.

and FITC-dex did not have significant effects on lung capillary endothelial surface area and/or ACE activity.

	PS (mL/min) (Start)	PS (mL/min) (End)
Normoxic lungs	17.5 ± 1.0	15.7 ± 1.2
Hyperoxic lungs	7.7 ± 0.5*	6.4 ± 0.2*

TABLE 2 Lung angiotensin converting enzyme (ACE) activity at the start and end of the bolus injection protocol.

PS (permeability–surface area product), which is a measure of lung ACE activity and an index of perfused capillary surface area for normoxic (n = 9) and hyperoxic (n = 5) rat lungs. Values are mean ± SE.

*Significantly different between normoxic and hyperoxic lungs (t-test; $p < 0.05$).

Figure 1 shows examples of venous effluent concentrations of FITC-dex and CoQ_1H_2 after their bolus injection into the arterial inlet of a normoxic lung (panel a) and a hyperoxic lung (panel b) perfused with three different BSA concentrations. The FITC-dex outflow curve indicates what the CoQ_1H_2 outflow curve would have looked like had the CoQ_1H_2 not interacted with the lung as it passed through the pulmonary vasculature. For the normoxic lung (panel a), the CoQ_1H_2 curves are shifted to the right and more dispersed than the FITC-dex curve, consistent with rapid equilibration of CoQ_1H_2 between the perfusate and the lung tissue on its passage through the pulmonary circulation.[2,3] Moreover, the CoQ_1H_2 curves show a progressive increase in the mean transit time of CoQ_1H_2, as indicated by the time position of the peak of the curve, on passage through the lung as perfusate BSA concentration decreased as predicted by Eq. (1). For the hyperoxic lung (panel b), the CoQ_1H_2 curves are also more dispersed than the FITC-dex curve, and the mean transit time of CoQ_1H_2 increased as the perfusate BSA concentration decreased. However, for the hyperoxic lung, the peaks of the CoQ_1H_2 curves are less shifted to the right relative to the peak of the FITC-dex curve as compared to the normoxic lung.

Annals of Biomedical Engineering, Vol. 38, No. 11 (November 2010): pg. 3449-3465. DOI.

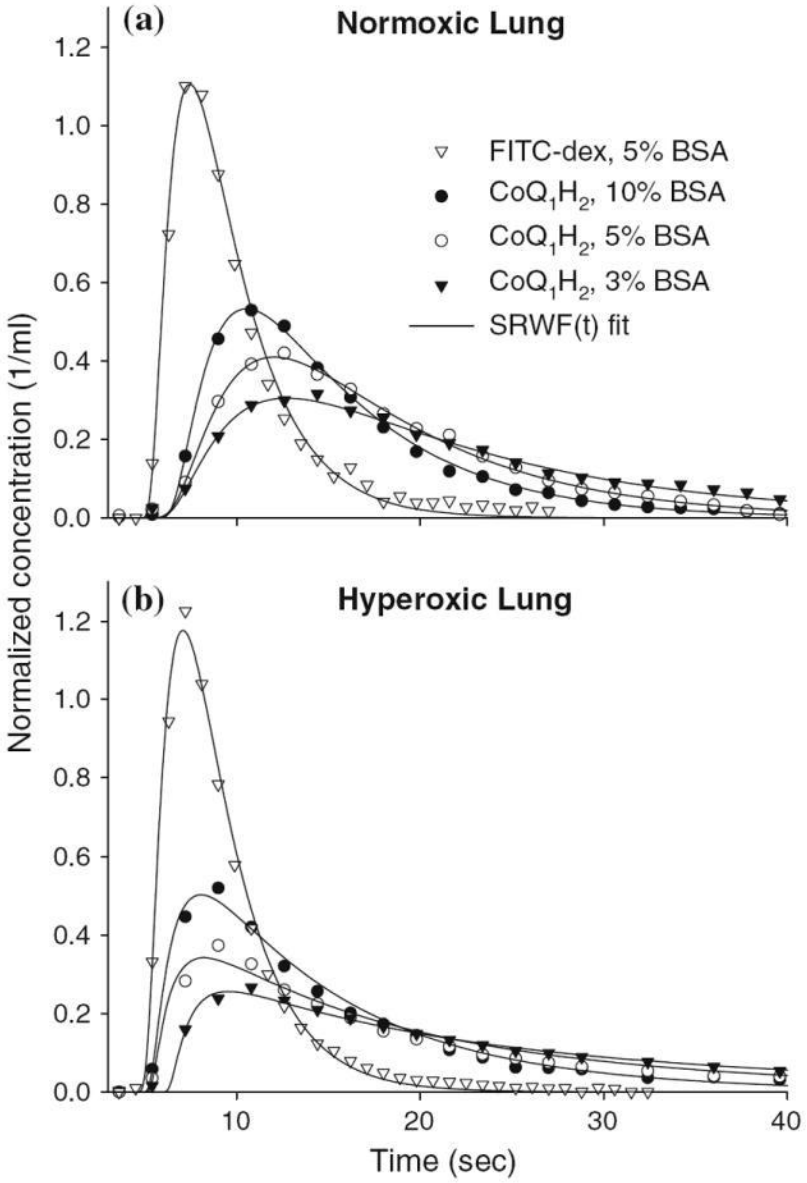

FIGURE 1 Venous effluent FITC-dex and CoQ_1H_2 normalized concentration (as a fraction of the injected amount per milliliter of effluent perfusate) vs. time data following the bolus injection of the indicators upstream from the pulmonary artery of a normoxic (panel a) and a hyperoxic (panel b) lung perfused with different perfusate %BSA concentrations. Lungs were treated with potassium cyanide (KCN) prior to bolus injections to inhibit mitochondrial complex III-mediated CoQ_1H_2 oxidation on passage through the lung. Solid lines are SRWF(t) fits.

Perfusion pressures for hyperoxic lungs in the absence or presence of papaverine were not significantly different from the corresponding pressures for normoxic lungs over the range of flows

Annals of Biomedical Engineering, Vol. 38, No. 11 (November 2010): pg. 3449-3465. DOI.

studied (Fig. 2). Moreover, for normoxic and hyperoxic lungs, perfusion pressure in the presence of papaverine was lower than that in the absence of papaverine over the range of flows studied. For each group of lungs, the effect of papaverine on perfusion pressure did not change over the range of flows studied, and was not different between normoxic (1.1 ± 0.05 (SD) Torr) and hyperoxic (1.1 ± 0.04 (SD) Torr) lungs. Change in perfusate %BSA had no effect on lung perfusion pressure at 10 mL/min for normoxic and hyperoxic lungs (data not shown). These results suggest that rat exposure to hyperoxic did not have significant effect on the distensibility or vasodilatory properties of the pulmonary vascular bed.

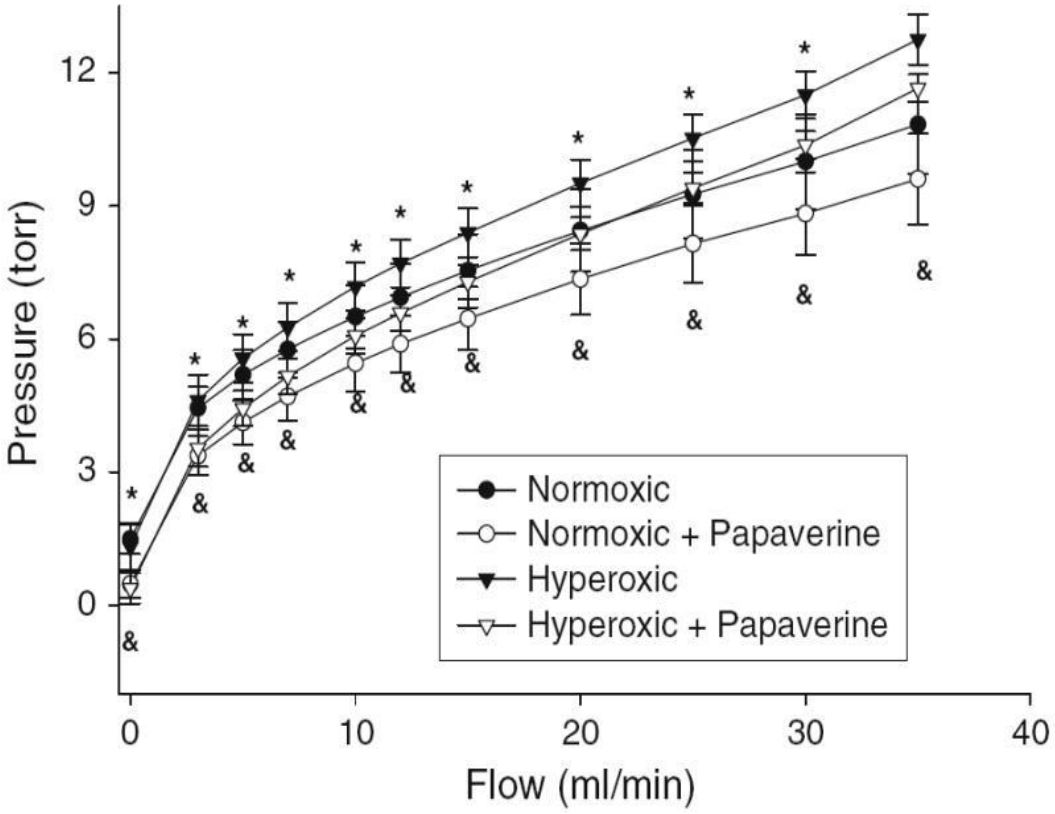

FIGURE 2 Arterial pressure-flow data from normoxic (*n* = 3) and hyperoxic (*n* = 3) lungs before (closed symbols) and after (open symbols) lung treatment with papaverine. (&) and (*) significantly different before and after lung treatment with papaverine for normoxic and hyperoxic lungs, respectively. Values are mean ± SE.

Annals of Biomedical Engineering, Vol. 38, No. 11 (November 2010): pg. 3449-3465. DOI.

DATA ANALYSIS

Moments of Co_1QH_2 and FITC-dex Outflow Curves

The mean transit time ($\bar{t}$) and variance (σ^2) of each FITC-dex and CoQ_1H_2 outflow curve ($C(t)$) were determined using a model-based approach in order to minimize the effect of noise in the tail.[6,8] Thus, for a given $C(t)$, $\bar{t}$ and σ^2 were obtained by fitting a shifted random walk function (SRWF(t)) to C(t). SRWF(t) is a probability density function whose functional form is defined by Eq. (3),[7]

$$\mathrm{SRWF}(t) = 0 \text{ for } t \le t_s, \quad \text{and } \left(\frac{\sqrt{\frac{\theta\phi}{4\pi(t-t_s)}}}{\theta} \exp\left(\frac{-\phi\left(1-\frac{(t-t_s)}{\theta}\right)}{4\frac{(t-t_s)}{\theta}} \right) \right) \text{ for } t > t_s \tag{3}$$

where

$\int_0^\infty \mathrm{SRWF}(t)\,dt = 1$ and Eqs. (4a) and (4b) relate θ, ϕ and t_s to $\bar{t}$ and σ^2.

$$\bar{t} = \theta\left(1+\frac{2}{\phi}\right) + t_s \tag{4a}$$

$$\sigma^2 = \frac{2\phi+8}{(\phi+2)^2}(\bar{t}-t_s)^2 \tag{4b}$$

The fitting procedure consists of determining the values of θ, ϕ, and t_s for which Eq. (3), scaled by the inverse of the perfusate flow (F), best fits $C(t)$ in the least squares sense. This procedure was implemented in MATLAB 7.0.1 using function '*lsqcurvefit*', (The MathWorks, Inc.). The coefficient of variation (CV), a measure of the goodness of fit (see "List of Symbols") between the measured outflow curve ($C(t)$) and the model SRWF(t) fit, was on average 12.2% for FITC-dex and 12.6% for CoQ_1H_2.

Annals of Biomedical Engineering, Vol. 38, No. 11 (November 2010): pg. 3449-3465. DOI.

The CoQ_1H_2 extravascular mean residence time ($\bar{t}_e$) at a given perfusate BSA concentration was determined by subtracting the mean transit time of the FITC-dex outflow curve ($C_R(t)$) from that for the CoQ_1H_2 outflow curve ($C_F(t)$) measured with the lung connected to the ventilation–perfusion system (Fig. 1), i.e.,

$$\bar{t}_e = \bar{t}_F - \bar{t}_R \qquad (5)$$

where $\bar{t}_R$ and $\bar{t}_F$ are the mean transit times of $C_R(t)$ and $C_F(t)$, respectively, determined as described above.

Evaluation of the Assumption of Rapidly Equilibrating Interactions of CoQ_1H_2 with Plasma Albumin (BSA) and with Lung Tissue

Equation (1) provides a relationship between the extravascular mean residence time ($\bar{t}_e$) and perfusate albumin concentration [BSA] for a diffusible test indicator for the case in which both (1) equilibration between perfusate and tissue of the free (i.e., not bound to plasma albumin) form of the indicator, and (2) association–dissociation of the indicator with plasma protein and lung tissue occur rapidly in comparison to the capillary mean transit time.[6,8] Algebraic manipulation of Eq. (1) results in Eq. (6)

$$\frac{1}{\bar{t}_e F} = \frac{1}{MQ_t} + \left(\frac{1}{MQ_t}\right)\frac{[BSA]}{K} \qquad (6)$$

Using the previously estimated value of K^{-1} for CoQ_1H_2 of 3.8 per %[BSA],[9] Eq. (6) is a oneparameter linear model for $1\bar{t}_eF$ with slope and intercept both equal to $1/MQ_t$. Equation (6) was fit to the mean values of $1\bar{t}_eF$ vs. [BSA]K for the normoxic and hyperoxic lungs separately (Fig. 3). The ability of Eq. (6) to fit the data in Fig. 3 reasonably well supports the assumption of rapidly equilibrating interactions of CoQ_1H_2 with perfusate BSA and normoxic and hyperoxic lung tissue.[6,8]

Annals of Biomedical Engineering, Vol. 38, No. 11 (November 2010): pg. 3449-3465. DOI.

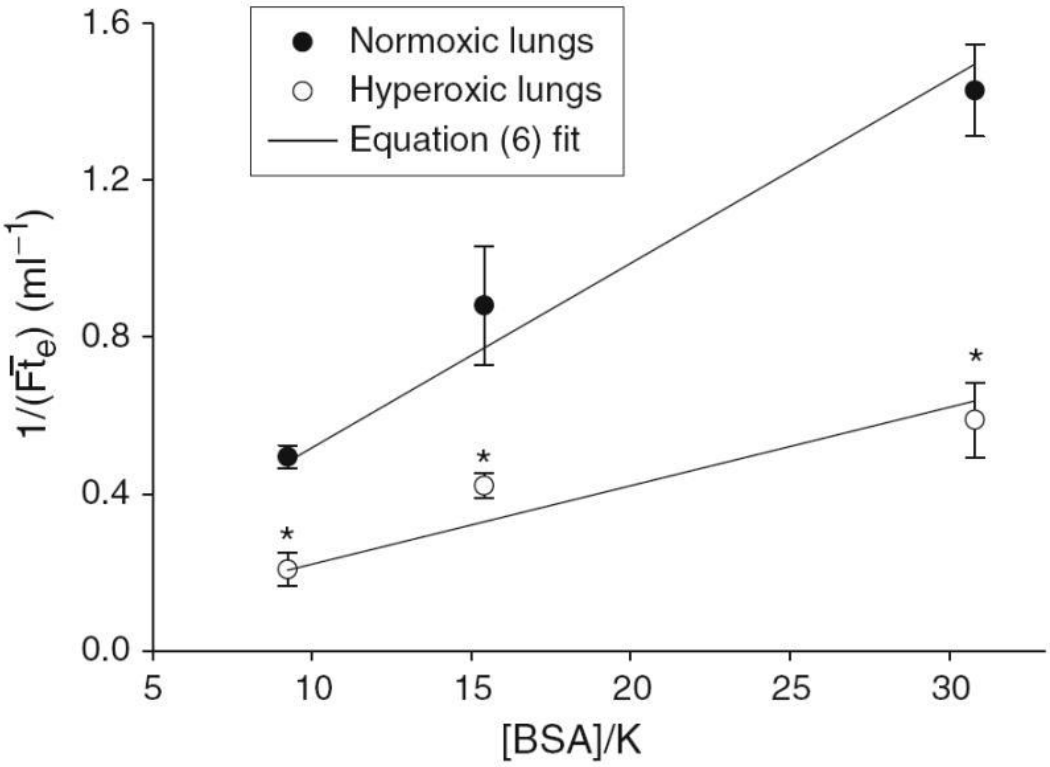

FIGURE 3 Symbols are data from normoxic (n = 6) and hyperoxic (n = 5) rat lung experiments plotted according to Eq. (6). K^{-1} was 3.8/%BSA.[9] $\bar{t}_e$ and F are the extravascular mean residence time and perfusate flow, respectively. Solid lines are Eq. (6) fit to data, resulting in a slope = intercept = 4.7 × 10^{-2} mL^{-1} for normoxic lungs (r^2 = 0.98) and 2.0 × 10^{-2} mL^{-1} for hyperoxic lungs (r^2 = 0.85).

Rat exposure to hyperoxia increased the value of $\bar{t}_e$ for CoQ_1H_2 at all three perfusate BSA concentrations studied (Fig. 3). For instance, the value of $\bar{t}_e$ at a perfusate BSA of 5% for hyperoxic lungs was 73% larger than that for normoxic lungs (Table 3). This increase in $\bar{t}_e$ could be due to a hyperoxia-induced increase in lung wet weight (Table 1) and/or increase in CoQ_1H_2 tissue-to-perfusate partition coefficient (M).

	$\bar{t}_v$ (s)	σ_v^2 (s^2)	RD_v	Q_v (mL)	$\bar{t}_e$ (s)
Normoxic	4.18 ± 0.26	4.05 ± 0.63	0.47 ± 0.02	0.70 ± 0.04	8.46 ± 0.66
Hyperoxic	3.29 ± 0.17*	2.82 ± 0.52	0.50 ± 0.04	0.55 ± 0.03*	14.64 ± 1.32*

Annals of Biomedical Engineering, Vol. 38, No. 11 (November 2010): pg. 3449-3465. DOI.

TABLE 3 Lung vascular mean transit time, variance and relative dispersion of vascular transit times, vascular volume, and CoQ_1H_2 extravascular mean residence time.

$\bar{t}_v$, $\sigma 2v$, RD_v, and Q_v are lung vascular mean transit time, variance of vascular transit times, relative distribution of vascular transit times, and vascular volume, respectively. $\bar{t}_e$ is the extravascular mean residence time of CoQ_1H_2 on passage through lungs perfused with 5% BSA perfusate. n = 9 (normoxic) and 5 (hyperoxic) for all parameters except $\bar{t}_e$ for which n = 7 for normoxic lungs. Values are mean ± SE.

*Significantly different between normoxic and hyperoxic lungs (t-test; $p < 0.05$).

Lung Total Vascular Volume and Vascular Transit Time Distribution

The lung vascular mean transit time ($\bar{t}_v$) and variance $\sigma 2v$ were obtained by finding the difference between the mean transit times and variances of the FITC-dex curves measured with ($C_R(t)$) and without (tubing; $C_{tub}(t)$) the lung in place in the ventilation–perfusion system, i.e.,

$$\bar{t}_v = \bar{t}_R - \bar{t}_{tub} \tag{7}$$

$$\sigma_v^2 = \sigma_R^2 - \sigma_{tub}^2. \tag{8}$$

The lung vascular volume (Q_v) was then determined as the product of $\bar{t}_V$ and the perfusate flow (F),

$$Q_v = \bar{t}_V F \tag{9}$$

The vascular relative dispersion (RD_v), a dimensionless measure of the heterogeneity of the lung vascular transit time distribution, was calculated as

$$RD_v = \sqrt{\sigma_V^2} / \bar{t}_V. \tag{10}$$

Annals of Biomedical Engineering, Vol. 38, No. 11 (November 2010): pg. 3449-3465. DOI.

Rat exposure to hyperoxia decreased vascular volume by an average of 21%, with no significant effect on $\boldsymbol{\sigma}_V^2$ or RD_v (Table 3).

Lung Capillary Mean Transit Time and Distribution of Capillary Transit Times

The MID method developed by Audi *et al*. for estimating the lung capillary transit time distribution ($h_c(t)$) is based on the following equations which relate the mean transit time, variance, and skewness of the measured outflow curves of the intravascular indicator ($C_R(t)$) and the flow-limited indicator ($C_F(t)$) to those of $h_c(t)$ ($\bar{t}_C$, $\boldsymbol{\sigma}_C^2$, and $\mathbf{m}_C^3$)[6,8]:

$$\sigma_{\mathrm{F}}^2 - \sigma_{\mathrm{R}}^2 = \left(\left(1 + \frac{\bar{t}_{\mathrm{e}}}{\bar{t}_{\mathrm{c}}}\right)^2 - 1\right) \sigma_{\mathrm{c}}^2 \tag{11a}$$

$$m_{\mathrm{F}}^3 - m_{\mathrm{R}}^3 = \left(\left(1 + \frac{\bar{t}_{\mathrm{e}}}{\bar{t}_{\mathrm{c}}}\right)^3 - 1\right) m_{\mathrm{c}}^3. \tag{11b}$$

Previous studies have demonstrated that >90% of the variance of the lung vascular transit time distribution ($\boldsymbol{\sigma}_V^2$) in a dog lung lobe, rabbit lung, and rat lung was due to the capillary bed.[2,6,8,20] Thus, algebraic manipulation of Eq. (11a), after substituting $\boldsymbol{\sigma}_V^2$ (Table 3) for $\boldsymbol{\sigma}_C^2$, leads to the following relationship between $\bar{t}_C$ and the extravascular moments of $C_F(t)$),[6,8]

$$\bar{t}_{\mathrm{c}} = \frac{\bar{t}_{\mathrm{e}}}{\sqrt{1 + \frac{\sigma_{\mathrm{e}}^2}{\sigma_{\mathrm{v}}^2} - 1}}, \tag{12}$$

where $\boldsymbol{\sigma}_e^2 = \boldsymbol{\sigma}_F^2 - \boldsymbol{\sigma}_R^2$. Model simulations (see "Discussion" section) were used to evaluate the impact of this assumption on the estimated value

Annals of Biomedical Engineering, Vol. 38, No. 11 (November 2010): pg. 3449-3465. DOI.

of $\bar{t}_C$. For this study, Eq. (12) was used to estimate $\bar{t}_C$ under the assumption that $\boldsymbol{\sigma}_C^2$ is equal to $\boldsymbol{\sigma}_V^2$ (Table 3).

The CoQ_1H_2 outflow curves measured using the three different perfusate BSA concentrations (Fig. 1) are analogous to outflow curves of three different flowlimited indicators each with a different $\bar{t}_e$ value. Thus, the moments of each of these outflow curves can be used in Eq. (12) to obtain three independent estimates of $\bar{t}_C$. Using this approach, the results in Table 4 show that perfusate BSA concentration had no significant effect on the estimated values of $\bar{t}_C$ and RD_c in either the normoxic or the hyperoxic lungs. This result suggests that the estimated values of $\bar{t}_C$ and RD_c are insensitive to the extravascular mean residence times of CoQ_1H_2 on its passage through either normoxic or hyperoxic lungs (Table 4). The results in Table 4 also show that the estimated value of $\bar{t}_C$ was 42% lower for hyperoxic lungs as compared to those for normoxic lungs. Moreover, the estimated value of the capillary relative dispersion $RD_C = \sqrt{\boldsymbol{\sigma}_V^2} / \bar{t}_C$, a dimensionless measure of the heterogeneity of $h_c(t)$, was 40% higher for hyperoxic lungs as compared to normoxic lungs.

	3% BSA		5% BSA		10% BSA	
	$\bar{t}_c$ (s)	RD_c	$\bar{t}_c$ (s)	RD_c	$\bar{t}_c$ (s)	RD_c
Normoxic	2.45 ± 0.37	0.82 ± 0.05	2.44 ± 0.33	0.78 ± 0.03	2.59 ± 0.29	0.77 ± 0.02
Hyperoxic	1.45 ± 0.15*	1.14 ± 0.01*	1.44 ± 0.16*	1.15 ± 0.02*	1.41 ± 0.15*	1.17 ± 0.03*

TABLE 4 Estimated values of the capillary mean transit time and relative dispersion as a function of perfusate %BSA concentration.

$\bar{t}_C$ and RD_c are the pulmonary capillary mean transit time and relatively dispersion of the capillary transit time distribution, respectively. Values are mean ± SE. n = 6 and 5 for normoxic and hyperoxic lungs, respectively. $\bar{t}_C$ was estimated using Eq. (12).

*Significantly different between normoxic and hyperoxic lungs (t-test; $p < 0.05$).

One way of evaluating the assumption that the variance of the total vascular transit time distribution (σ2v) is due to the capillary bed, i.e., $\boldsymbol{\sigma}_C^2=\boldsymbol{\sigma}_V^2$, is to rearrange Eq. (11a) to obtain the following relationship between $\bar{t}_e$ and $\boldsymbol{\sigma}_e^2$

$$\sigma_e^2 = \frac{\sigma_v^2}{\bar{t}_c^2}\bar{t}_e^2 + 2\frac{\sigma_v^2}{\bar{t}_c}\bar{t}_e \qquad (13)$$

containing the one unknown parameter $\bar{t}_c$. The ability of Eq. (13) to fit the $\bar{t}_e$ vs. σ2e data (Fig. 4) for the normoxic and hyperoxic bolus injection data is consistent with the above assumption. Table 5 shows that the values of $\bar{t}_c$ estimated using Eq. (13) for normoxic and hyperoxic lungs are virtually the same as those estimated using Eq. (12) (Table 4).

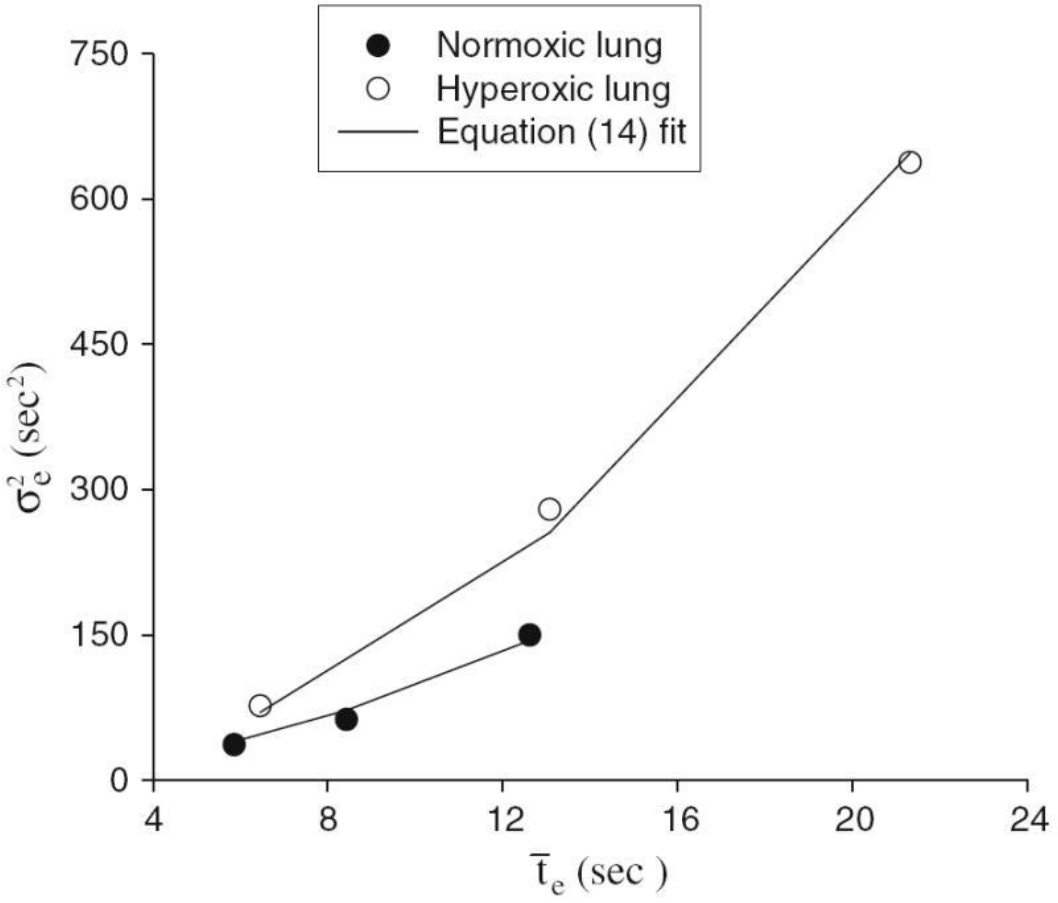

Annals of Biomedical Engineering, Vol. 38, No. 11 (November 2010): pg. 3449-3465. DOI.

FIGURE 4 Symbols are data from the outflow curves shown in Fig. 1 plotted according to Eq. (13). $\bar{t}_e$ and σ_e^2 are CoQ_1H_2 extravascular mean residence time and variance, respectively. Solid lines are Eq. (13) fit to the normoxic (r^2 = 0.99) and hyperoxic (r^2 = 0.98) data.

	$\bar{t}_c$ (s)	RD_c	Q_c (mL)	Q_c/Q_v
Normoxic	2.45 ± 0.26	0.82 ± 0.03	0.41 ± 0.04	0.58 ± 0.04
Hyperoxic	1.43 ± 0.15*	1.15 ± 0.01*	0.24 ± 0.03*	0.43 ± 0.04*

TABLE 5 Estimated values of lung capillary mean transit time, volume, and relative dispersion of the capillary transit time distribution.

$\bar{t}_C$, RD_c, and Q_c are lung capillary mean transit time, relative dispersion of the capillary transit time distribution, and lung capillary volume, respectively. Q_v is lung vascular volume. $\bar{t}_C$ was estimated using Eq. (13). Values are mean ± SE. n = 6 and 5 for normoxic and hyperoxic lungs, respectively.

*Significantly different between normoxic and hyperoxic lungs (t-test; $p < 0.05$).

A random walk function (Eq. 3) was used to approximate the functional shape of the capillary transit time distribution using the average of the estimated values of the capillary mean transit times and variances (Tables 3 and and5).5). The resulting approximations for the normoxic and hyperoxic $h_c(t)$ curves are shown in Fig. 5.

Annals of Biomedical Engineering, Vol. 38, No. 11 (November 2010): pg. 3449-3465. DOI.

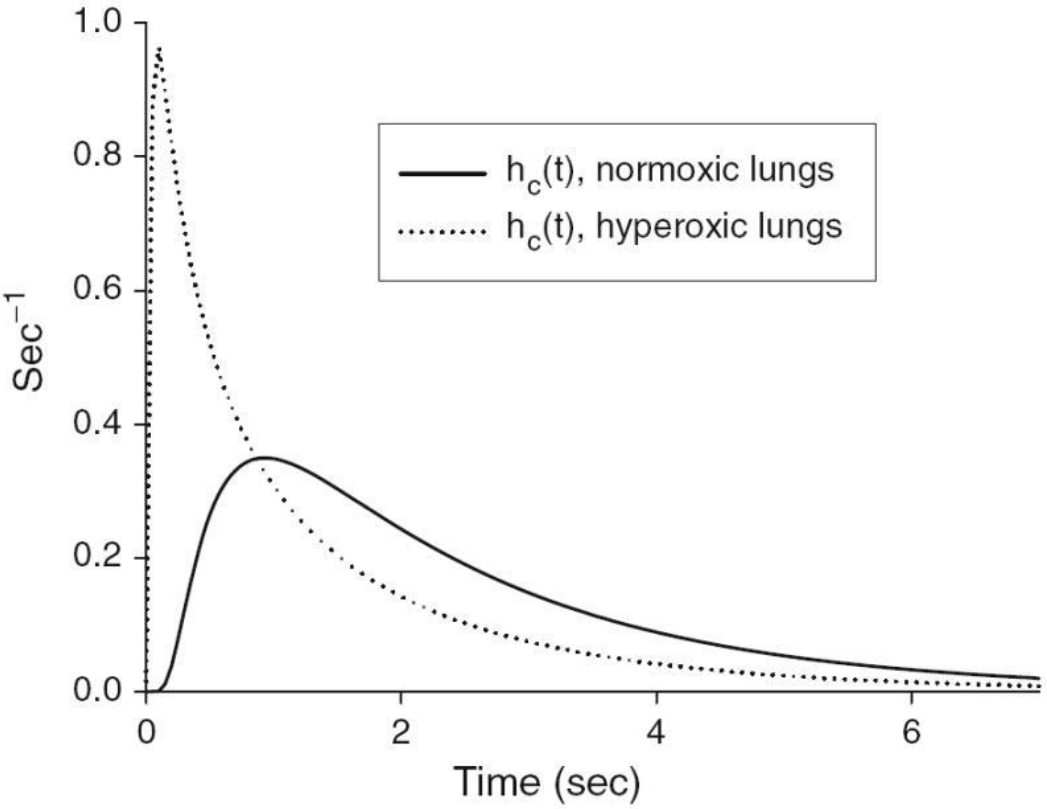

FIGURE 5 Approximation of the functional form of the capillary transit time distribution ($h_c(t)$) for normoxic and hyperoxic lungs using a shift random walk function (Eq. 3) with the shift (t_s) set to zero (see text).

DISCUSSION

The objective of this study was to evaluate the effect of rat exposure to hyperoxia (85% O_2 for 7 days) on capillary mean transit time and capillary transit time distribution in the intact rat lung using the MID method developed by Audi *et al*. with CoQ_1H_2 as the flow-limited indicator and FITC-dex as the intravascular indicator.[6,8] The results demonstrate that rat exposure to this hyperoxia model decreases $\bar{t}_C$ by 42% and increases the relative dispersion of $h_c(t)$ by 40%.

For comparison, Table 6 summarizes previous estimates of $\bar{t}_C$, RD_c, and capillary volume ($Q_c = F\bar{t}_C$) of the normoxic rat lung. To put these

Annals of Biomedical Engineering, Vol. 38, No. 11 (November 2010): pg. 3449-3465. DOI.

results in perspective, it is useful to compare Q_c values since it is less dependent on flow than is $\bar{t}_C$. Table 6 shows that capillary volume estimated in this study is close to that estimated by Audi *et al*.[2] with ^{3}H-alfentanil and ^{14}C-diazepam as the flow-limited indicators, and to capillary volume estimated by Presson *et al*.[47] using subpleural fluorescence video-microscopy under similar flow conditions. However, Table 6 shows that previous morphometric estimates of capillary volume (0.58–0.71 mL) are higher than that estimated in this study or using subpleural vessel fluorescence video-microscopy.[21,48,52] This is not surprising since reported morphometric estimates of capillary volume have been considered to be close to their maximum value, which might not be achieved under the low-flow, low-pressure conditions in this study.[6,8]

Method	Body wt. (g)	Q_c (mL)	Q_c (mL/kg Body wt.)	Flow (mL/min)	$\bar{t}_c$ (s)	RD_c	Reference
Morphometric	307 ± 11	0.63 ± 0.07	2.10				Crapo *et al.*[22]
Morphometric	363 ± 4	0.66 ± 0.06	1.82				Crapo *et al.*[21]
Morphometric	366 ± 4	0.71 ± 0.06	1.94				Sjostrom and Crapo[52]
Morphometric	224	0.58 ± 0.05	2.6				Randell *et al.*[48]
Fluorescence microscopy	360–580	0.49 ± 0.03	1.04	7.5	3.9 ± 0.2	0.57 ± 0.02	Presson *et al.*[47]
Morphometric	306 ± 5	0.51 ± 0.05	1.67				Howell *et al.*[36]
Method A	323 ± 6	0.47 ± 0.02	1.46	30	0.94 ± 0.04	0.91 ± 0.03	Audi *et al.*[2]
Present method	302 ± 9	0.41 ± 0.04	1.36	10	2.54 ± 0.24	0.82 ± 0.03	Present study

TABLE 6 Estimates of pulmonary capillary mean transit time and blood volume for rat lungs in chronological order.

Estimates of pulmonary capillary blood volume (Q_c), mean transit time ($\bar{t}_c$), and relative dispersion (RD_c) of $h_c(t)$. Values are mean ± SE.

The estimated relative dispersion of the capillary transit time distribution for normoxic lungs of 0.82 ± 0.03 (SE) in this study (Table 5) is similar to that estimated by Audi *et al*.[2] using ^{3}H-alfentanil and ^{14}C-diazepam as the flow-limited indicators (0.91), but smaller than that estimated using subpleural vessel fluorescence video-microscopy (0.57) under similar flow conditions (Table 6).[47] This could be due in part to morphometric differences between the subpleural and intrapulmonary capillary beds,[33,45] although Presson *et al*. suggested that these differences might not be significant for the rat lung.[47]

Rat exposure to hyperoxia (85% O_2 for 7 days) decreased the lung capillary volume (and hence capillary mean transit time) by 42% from 0.41 ± 0.04 (SE) to 0.24 ± 0.03 mL (Table 5). This result is consistent with that measured by Crapo *et al*. using a morphometric method.[21] There they showed that this hyperoxic model resulted in the loss of large sections of the pulmonary capillary bed and decreased the pulmonary capillary volume by ~50%, from 0.63 to 0.32 mL.[21,22]

The hyperoxia-induced decrease in lung capillary volume is also consistent with the hyperoxia-induced 56% decrease in the rate (PS) of ACE-mediated FAPGG hydrolysis measured in this study (Table 2). Assuming no change in ACE activity per unit surface area between normoxic and hyperoxic lungs, the change in PS (Table 2) would be proportional to the change in perfused surface area.[2,9] This 56% hyperoxia-induced decrease in PS product (Table 2) is consistent with the 50% decrease in surface area of the capillary endothelium measured by Crapo *et al*. using morphometric methods (4524 cm^2 vs. 2289 cm^2).[21,22]

Exposure of rats to hyperoxia decreased total lung vascular volume by 21%, with no significant effect on relative dispersion of lung vascular transit time distribution (Table 3). This hyperoxia-induced decrease in vascular volume (0.15 mL) (Table 3) is comparable to the hyperoxia-induced decrease in capillary volume (0.17 mL) (Table 5). This suggests that exposure to hyperoxia had no significant effect on the volume of the conducting vessels of the lung. As a result, capillary volume as a percentage of the vascular volume decreased from 58 ± 4 (SE)% in normoxic lungs to 43 ± 4% in hyperoxic lungs (Table 5).

The results of this study demonstrate that rat exposure to hyperoxia not only decreased the capillary volume, but also increased the relative dispersion of $h_c(t)$ by 40% from 0.82 ± 0.03 (SE) to 1.15 ± 0.01 for normoxic and hyperoxic lungs, respectively. To our knowledge, this is the first study to evaluate the effect of rat exposure to 85% O_2 for 7 days on the heterogeneity of $h_c(t)$. This hyperoxia-induced increase in RD_c is revealed in the measured CoQ_1H_2 and FITC-dex outflow curves (Fig. 1) as a decrease in the shift of the time positions of the peaks of CoQ_1H_2 outflow curves relative to that of the FITC-dex curve as demonstrated by the model simulations described below.

Annals of Biomedical Engineering, Vol. 38, No. 11 (November 2010): pg. 3449-3465. DOI.

The estimated values of $\bar{t}_c$ and the relative dispersion (RD_c) of $h_c(t)$ using Eq. (12) are independent of the extravascular volume of the rapidly equilibrating indicator. This is consistent with the results in Table 4 which show that the estimated values of $\bar{t}_c$ and RD_c are not sensitive to changes in perfusate BSA concentration, which alters the tissue–plasma partition coefficient of CoQ_1H_2 and its apparent extravascular volume (Fig. 3). Thus, the estimated hyperoxiainduced decrease in $\bar{t}_c$ and increase in RD_c cannot be explained by the larger extravascular volume of distribution (dilution effect) of CoQ_1H_2 in hyperoxic lungs. Similar changes in $\bar{t}_c$ and RD_c would be expected using Eq. (12) with other flow-limited indicators.

The estimated distributions of capillary transit times in normoxic and hyperoxic lungs result from distributions of capillary flows, diameters, lengths, or combinations thereof.[6-8] Separating the relative contribution of capillary flows vs. geometries to the distribution of capillary transit times requires additional information not available in the indicator dilution data themselves.[7]

The functional form of $h_c(t)$ for normoxic and hyperoxic lungs was approximated using a shifted random walk function (Fig. 5) with the shift (minimum capillary transit time) set to zero since additional information such as skewness of $h_c(t)$ would be needed to determine this shift.[6-8] Other right-skewed functions that have been used to approximate the functional form of $h_c(t)$ include the lagged normal density function and a time-shifted exponential function.[6-8,12] For this study, the shifted random walk function was chosen since it provided a good fit to the measured FITC-dex and CoQ_1H_2 concentration vs. time outflow curves as indicated by the relatively low coefficient of variations.

The pressure-flow experiments (Fig. 2) show that exposure to hyperoxia did not have a significant effect on the distensibility and vasodilatory properties of the pulmonary vascular bed. Thus, carrying out the MID experiments in the presence of papaverine and/or at a higher flow (and hence higher perfusion pressure) could have resulted in larger vascular and capillary volumes for normoxic and hyperoxic lungs, but would not have had a significant effect on the hyperoxiainduced % decrease in total vascular or capillary volume. This is consistent with the fact that the morphometrically measured

capillary volumes by Crapo *et al*. for normoxic (0.63 mL) and hyperoxic (0.32 mL) lungs are larger than those measured in this study (Table 5), but their hyperoxia-induced decrease in capillary volume (~50%) is close to that in this study (~42%).[21,22]

The rat lung capillary mean transit time reported in this study is plasma mean transit time, which is longer than that for red blood cells (RBC) because of the Fahraeus effect.[1,47] Presson *et al*. found the plasma mean transit time in subpleural capillaries of dog lungs to be ~40% longer than that for RBC.[46] Assuming similar capillary diameters in dog and rat lungs, and that the ratio of RBC velocity to plasma velocity in a lung capillary is flow independent, the estimated RBC mean transit time based on the results of this study would be ~0.25 s, which is close to the time needed for O_2 to diffuse and react with RBC.[47] This suggests that rat lungs have little reserve capillary RBC mean transit time.[47] This could be in part due to the fact that the estimated plasma capillary mean transit time in this study does not account for capillary distension due to difference in lung perfusion pressure at normal cardiac output (~75 mL/min for 300 g rat) as compared to 10 mL/min perfusate flow used in this study (Fig. 2). Generally speaking, RBC transit time is more relevant for gas exchange between blood and air, whereas plasma transit time is more relevant for substrate exchange between blood and tissue and for the subsequent evaluation of the effect of rat exposure to hyperoxia on the activities of redox enzymes in the intact lung using indicator dilution methods.

Exposure to hyperoxia increased aortic blood hematocrit by ~15% (Table 1), consistent with results of previous studies, which have suggested this increase could be due to dehydration.[21,22] Crapo *et al*. showed that unlike aortic blood hematocrit, morphometrically measured pulmonary capillary blood hematocrit was ~30% lower in hyperoxic lungs as compared to normoxic lungs.[21,22] They suggested that this decrease could be due to some type of obstruction in large segments of the pulmonary capillary bed that allowed plasma to flow through these capillaries, but not red blood cells (RBC), and that RBC would have had to bypass these sections of the pulmonary capillary bed and shunt through larger vessels.[21,22] This shunt is consistent with the fact that these animals show signs of peripheral cyanosis even in a hyperoxic environment. [21,22] Moreover, the existence of such shunt

Annals of Biomedical Engineering, Vol. 38, No. 11 (November 2010): pg. 3449-3465. DOI.

could explain the fraction of capillaries with relatively short transit times in hyperoxic lungs (Fig. 5) and the early appearance of CoQ_1H_2 on passage though hyperoxic lungs as compared to normoxic lungs (Fig. 1).

To demonstrate the effect of an increase in the heterogeneity of $h_c(t)$ on the shift between the peaks of the outflow curves of an intravascular indicator and a flow-limited indicator, a previously developed mathematical model (Appendix) was utilized to simulate the outflow curves of intravascular and flow-limited indicators following their arterial bolus injection into a normoxic and a hyperoxic lung. For the normoxic model simulation, the values of $\bar{t}_c$ and RD_c were set at 2.5 s and 0.8, respectively. For the hyperoxic model simulation, the value of RD_c was set at 1.2, while $\bar{t}_c$ was held at 2.5 s. Both model simulations used the same $\bar{t}_e$ values (4, 8, and 12 s to simulate CoQ_1H_2 outflow curves with 10, 5, and 3% perfusate BSA concentrations, respectively) and the same level of bolus dispersion outside the capillary bed (i.e., tubing and conducting vessels). Thus, the only difference between the normoxic and hyperoxic models was the increased RD_c value. Figure 6 shows the simulated outflow curves of the intravascular and flow-limited indicators from the normoxic (panel a) and hyperoxic (panel b) models. Increasing the RD_c of $h_c(t)$ in the hyperoxic model (panel b) decreased the shift between the peak of the intravascular outflow curve and the peaks of the flow-limited outflow curves by an amount comparable to the hyperoxia-induced decrease in the shift between the peaks of the measured outflow curves of FITC-dex and CoQ_1H_2 (Fig. 1).

Annals of Biomedical Engineering, Vol. 38, No. 11 (November 2010): pg. 3449-3465. DOI.

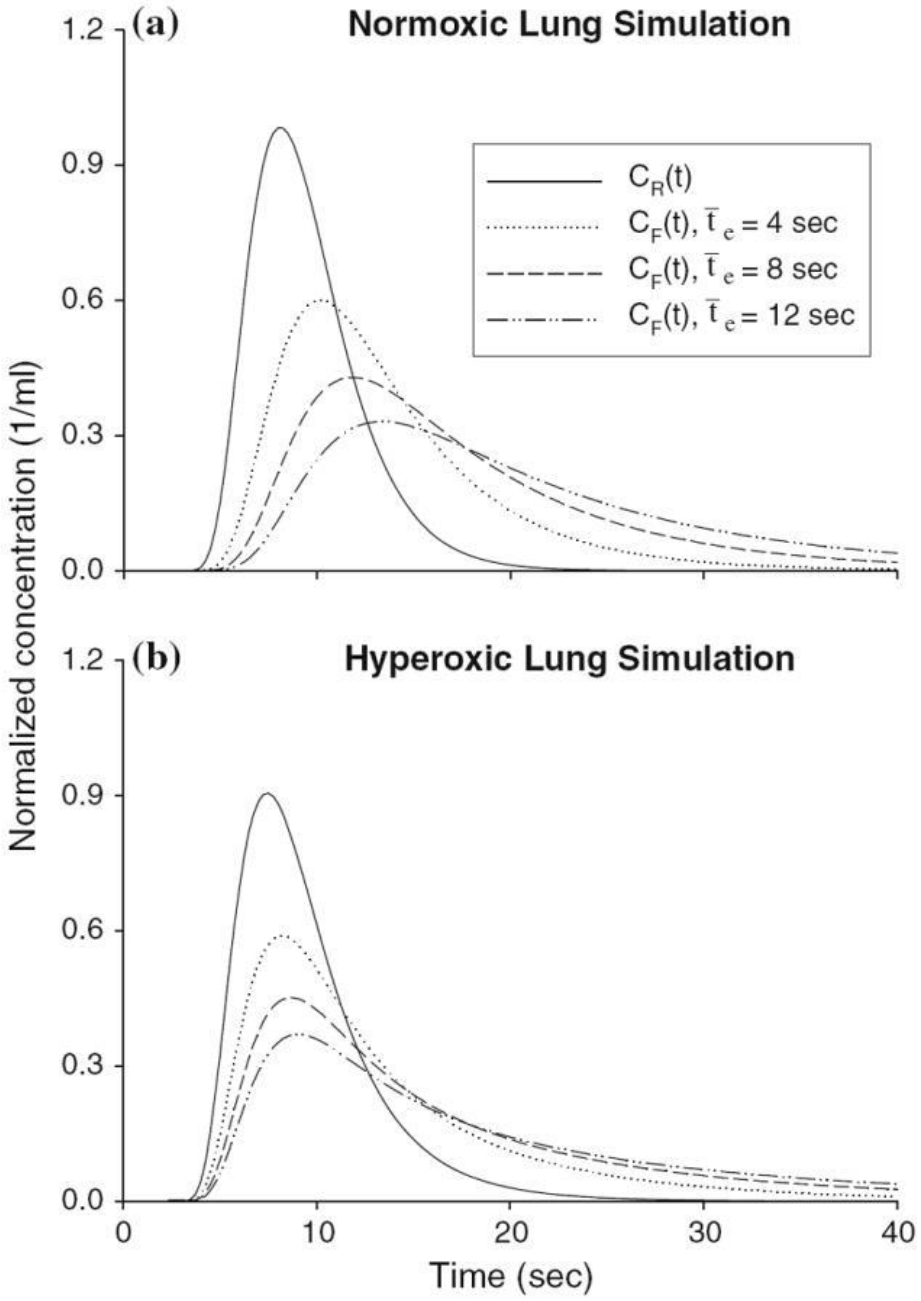

FIGURE 6 Simulations (see Appendix) of arterial bolus injections of an intravascular indicator ($C_R(t)$) and a flow-limited ($C_F(t)$) indicator with different extravascular mean residence times ($\bar{t}_e$) in a normoxic (panel a) and a hyperoxic (panel b) lung. The normoxic and hyperoxic model simulations are assumed to have the same bolus dispersion outside the capillary bed, same capillary mean transit time (2.5 s), but different capillary relative dispersion (RD_c = 0.8 and 1.2 for normoxic and hyperoxic lung simulations, respectively).

Annals of Biomedical Engineering, Vol. 38, No. 11 (November 2010): pg. 3449-3465. DOI.

The simulated outflow curves shown in Fig. 6 (panel a) were also used to evaluate the assumption of Eq. (12) that all of the variance of the bolus dispersion within the lung vasculature is due to the capillary bed, rather than to conducting vessel. The moments of each of the simulated outflow curves were calculated (Eq. 3) and then used in Eq. (12) to estimate $\bar{t}_c$ with $\boldsymbol{\sigma}_V^2$ set at (a) the actual value of $\boldsymbol{\sigma}_C^2$, (b) 1.1 times the actual value of $\boldsymbol{\sigma}_C^2$, (10% overestimation of $\boldsymbol{\sigma}_C^2$,), and c) 1.2 times the actual value of $\boldsymbol{\sigma}_C^2$, (20% overestimation of $\boldsymbol{\sigma}_C^2$,). Figure 7 shows the ratios of estimated (Eq. 12) to actual values of $\bar{t}_c$. Overestimation of σ2c by 10 and 20% resulted on average in overestimation of $\bar{t}_c$ by ~7 and ~15%, respectively, using Eq. (12).

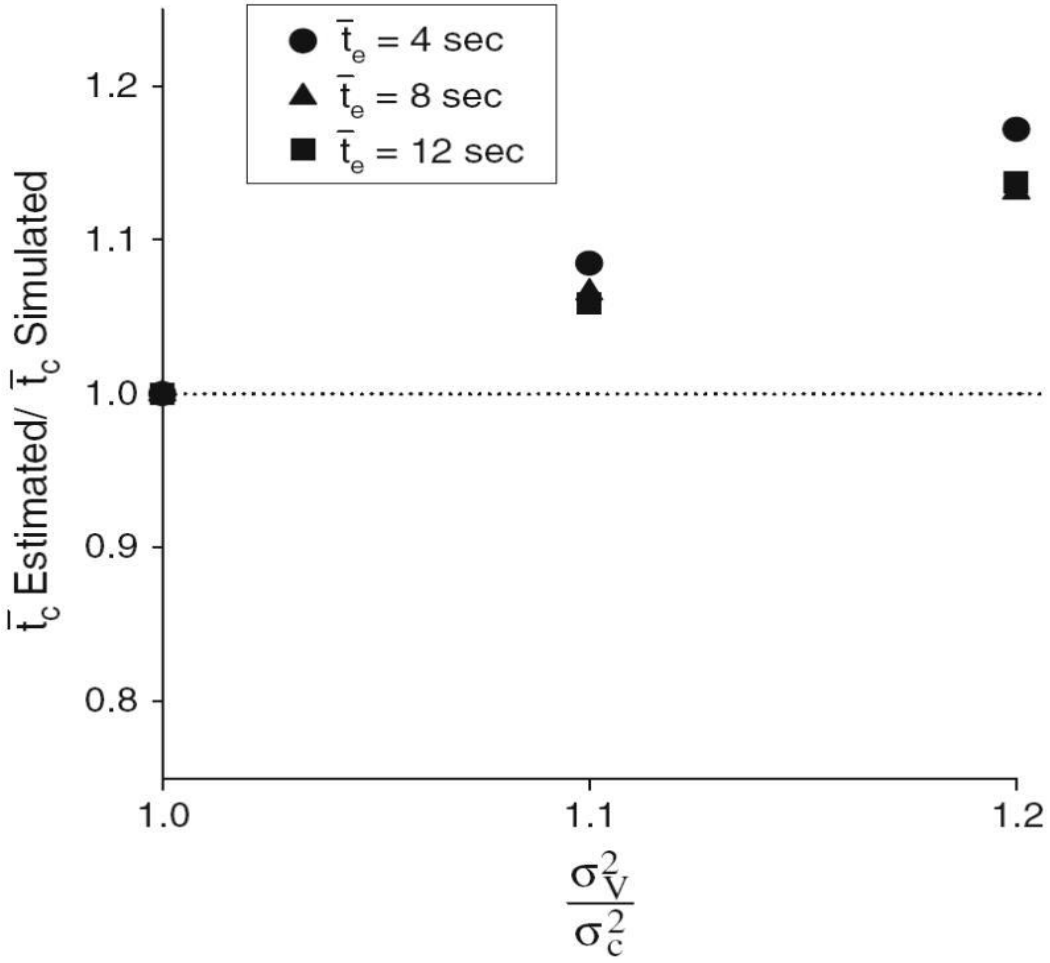

FIGURE 7 Ratio of estimated value (Estimated) of capillary mean transit time ($\bar{t}_c$) using Eq. (12) to that used in the simulations (Simulated) as a function of the ratio of

Annals of Biomedical Engineering, Vol. 38, No. 11 (November 2010): pg. 3449-3465. DOI.

total vascular variance ($\boldsymbol{\sigma}_V^2$,) to the capillary variance ($\boldsymbol{\sigma}_C^2$,) for three different extravascular mean residence times ($\bar{t}_e$). The values of $\bar{t}_c$ and $\boldsymbol{\sigma}_C^2$, used in the model simulations were 2.5 s and 4 s^2, respectively.

Equation (12) is equivalent to the superposition method developed by Goresky[32] as implemented by Audi *et al*.[8] Thus, one would expect the estimates of $\bar{t}_c$ obtained using the Goresky superposition method to be comparable to those obtained using Eq. (12) if the dispersion due to the tubing, injection, and sampling systems was removed from the FITC-dex and CoQ_1H_2 outflow curves before applying the superposition method.[8]

Comparison of the results from this study with previous results using the MID method developed by Audi *et al*. in the isolated perfused dog lung lobe and rabbit lungs reveals quantitative differences in the estimated vascular and capillary mean transit times among these species.[6,8] Assuming a normal cardiac output of 2.9 L/min for a 20-kg dog,[6] we estimated the pulmonary capillary and total pulmonary vascular mean transit times to be 1.62 and 3.40 s, respectively.[6] For a 2.7-kg rabbit with a normal cardiac output of 340 mL/min, the estimated pulmonary capillary and total pulmonary vascular mean transit times were 0.76 and 1.70 s, respectively.[8] Assuming a normal cardiac output of 75 mL/min for a-300 g rat,[47] the estimated pulmonary capillary and total pulmonary vascular mean transit times in this study, based on the results in Tables 5, would be 0.33 and 0.57 s, respectively. It is important to note that this estimate does not account for the effect of passive distension of blood vessels at this higher flow (Fig. 2). These transit times appear to be substantially shorter than those of the rabbit, which in turn are substantially shorter than those of the dog. However, the pulmonary capillary mean transit time as a percentage of the total vascular mean transit time appears to be similar for dogs (48%), rabbits (44%), and rats (58%). Thus, the shorter capillary mean transit time in the rat, as compared to those of the rabbit and dog, may be primarily attributed to the proportionately shorter total vascular mean transit time. Moreover, studies by Staub and Schultz[53] and Mercer and Crapo[42] show that the capillary length in rat lungs (~205 μm) was significantly shorter than in rabbit lungs (550–650 μm) and dog lungs (600–800 μm).

The pulmonary endothelium, which has a relatively large surface area and is in direct contact with blood-borne compounds, has the potential to influence the redox status and plasma concentrations of endogenous and exogenous blood-borne redox active compounds via cell surface and intracellular oxidoreductases.[2-5,9-11,16,17,24,43,44] This might include a range of pharmacological, physiological, and toxic redox active compounds (e.g., quinones).[2,9,18,41] The longer the capillary mean transit time, the more time available for redox active compounds to interact with the lung tissue on passage through the pulmonary circulation. Furthermore, the overall rate of substrate exchange between blood and tissue has been shown to be inversely proportional to the heterogeneity of $h_c(t)$.[2,7,31] Thus, the hyperoxia-induced decrease in $\bar{t}_c$ and increase in the heterogeneity of $h_c(t)$ measured in this study could alter the bioavailability and bioactivity of blood-borne redox-active compounds, and hence their pro- or anti-oxidant activity in lung tissue, blood vessels, and downstream organs. This is potentially important considering that the pulmonary endothelium is a primary target of lung O_2 toxicity.[21,23] Previously, we demonstrated using model simulations the impact of the heterogeneity of $h_c(t)$ on the rate of reduction of redox active test indicators on passage through the pulmonary capillary bed.[2]

The pulmonary capillary mean transit time and transit time distribution, $h_c(t)$, are important determinants of lung function in health and disease.[56] For instance, the effectiveness of lungs for providing adequate O_2 exchange between air and blood is dependent on the blood spending sufficient time in the pulmonary capillaries. In addition, even if the blood is in some capillaries for a long time (capillaries with long transit times), but spends too little time in others (capillaries with short transit times), a gas exchange deficit can occur. This is because the rapid transit of blood through capillaries with short transit times can never be compensated for by slow transit through capillaries with long transit times. Thus, the hyperoxia-induced decrease in capillary mean transit time and increase in the relative dispersion of capillary transit time distribution determined in this study have the potential to negatively affect the ventilation–perfusion ratio and even produce a gas exchange deficit.[22] This is consistent with the ~50% drop in the diffusion capacity of the lungs in these hyperoxic animals estimated morphometrically by Crapo *et al*., and the fact that

these animals experience peripheral cyanosis even in a hyperoxic environment.[21,22]

In conclusion, the results of this study demonstrate that estimates of the rat lung capillary transit time distribution can be obtained from the venous effluent concentration vs. time outflow curves of an intravascular indicator and one flow-limited indicator such as CoO_1H_2, measured following their arterial bolus injection. Furthermore, the results reveal that rat exposure to this hyperoxia model (85% O_2 for 7 days) decreased lung capillary mean transit time and increased the heterogeneity of the lung capillary transit time distribution. These results are important for subsequent evaluation of the effect of this unique hyperoxia model on the activities of endothelial pro- and anti-oxidant redox enzymes in the intact lung using indicator dilution methods, and for elucidation of the potential role of these enzymes in rat tolerance to 100% O_2 stimulated by pre-exposure to 85% O_2.[7]

Acknowledgments

We sincerely thank Mr. Robert Bongard for his help with the experiments. This study was supported by NIH grant HL-24349, and the Department of Veterans' Affairs.

LIST OF SYMBOLS

BSA	Bovine serum albumin
$h_c(t)$	Capillary transit time distribution
$C_R(t)$	Concentration (1/mL) of the intravascular reference indicator in the venous effluent at a time t following bolus injection at $t = 0$
$C_F(t)$	Concentration (1/mL) of the flow-limited indicator in the venous effluent at a time t following bolus injection at $t = 0$

$C_{tub}(t)$	Concentration (1/mL) of the intravascular indicator in the venous effluent at a time t following bolus injection (at t = 0) with the lung removed from the ventilation–perfusion system
CV	$\sum Mi=1(Ci-\mathrm{SRWF}i)2(M-\mathrm{Par})\sqrt{1M}\sum Mi=1Ci\times 100$ = Coefficient of variation between outflow curve (C) and shifted random walk (SRWF) fit (%). M and Par are number of data points fitted and number model parameters (3 for SRWF), respectively
FAPGG	Angiotensin converting enzyme substrate
$\bar{t}$	Mean transit time (the first moment) (s)
$\bar{t}_S$	Lung vascular mean transit time (s)
$\bar{t}_c$	Lung capillary mean transit time (s)
$\bar{t}_R$	Mean transit time of the intravascular indicator concentration vs. time outflow curve, $C_R(t)$ (s)
$\bar{t}_F$	Mean transit time of the flow-limited indicator concentration vs. time outflow curve, $C_F(t)$ (s)
$\bar{t}_{tub}$	Mean transit time of the tubing concentration vs. time outflow curve, $C_{tub}(t)$ (s)
$\bar{t}_e$	Extravascular mean residence time (s)
σ^2	Variance (second central moment) (s^2)
$\boldsymbol{\sigma_v^2}$	Variance of lung total vascular transit time distribution (s^2)
$\boldsymbol{\sigma_c^2}$	Variance of $h_c(t)$ (s^2)

Annals of Biomedical Engineering, Vol. 38, No. 11 (November 2010): pg. 3449-3465. DOI.

$\boldsymbol{\sigma_R^2}$	Variance of the intravascular indicator concentration vs. time outflow curve, $C_R(t)$ (s^2)
$\boldsymbol{\sigma_F^2}$	Variance of the flow-limited indicator concentration vs. time outflow curve, $C_F(t)$ (s^2)
$\boldsymbol{\sigma_e^2}$	σ2F−σ2R extravascular variance (s^2)
m^3	Skewness (third central moment) (s^3)
m^3_c	Skewness of $h_c(t)$ (s^3)
m^3_R	Skewness of the intravascular indicator concentration vs. time outflow curve (s^3)
m^3_F	Skewness of the flow-limited indicator concentration vs. time outflow curve (s^3)
Q_v	Lung vascular volume (mL)
Q_c	Lung capillary volume (mL)
Q_t	Lung tissue volume accessible to the flow-limited indicator from the vascular region (mL)
RD_v	Relative dispersion of the vascular transit time distribution
RD_c	Relative dispersion of the capillary transit time distribution
F	Perfusate flow (mL/min)
M	Tissue-to-plasma partition coefficient of the flow-limited indicator
K	Equilibrium dissociation constant of the binding of the flow-limited indicator with perfusate BSA

Annals of Biomedical Engineering, Vol. 38, No. 11 (November 2010): pg. 3449-3465. DOI.

PS	Permeability–surface area product (mL/min), which is a measure of lung angiotensin converting enzyme activity and an index of perfused capillary surface area
P_a	Lung perfusion pressure (Torr)

APPENDIX: MATHEMATICAL MODEL

Single Capillary Element The model utilized for this study has been described previously.[6,7] Briefly, each capillary element consists (Fig. 8) of a capillary region and a surrounding extravascular region, with volumes V_c and V_e, respectively. The model assumes the following:

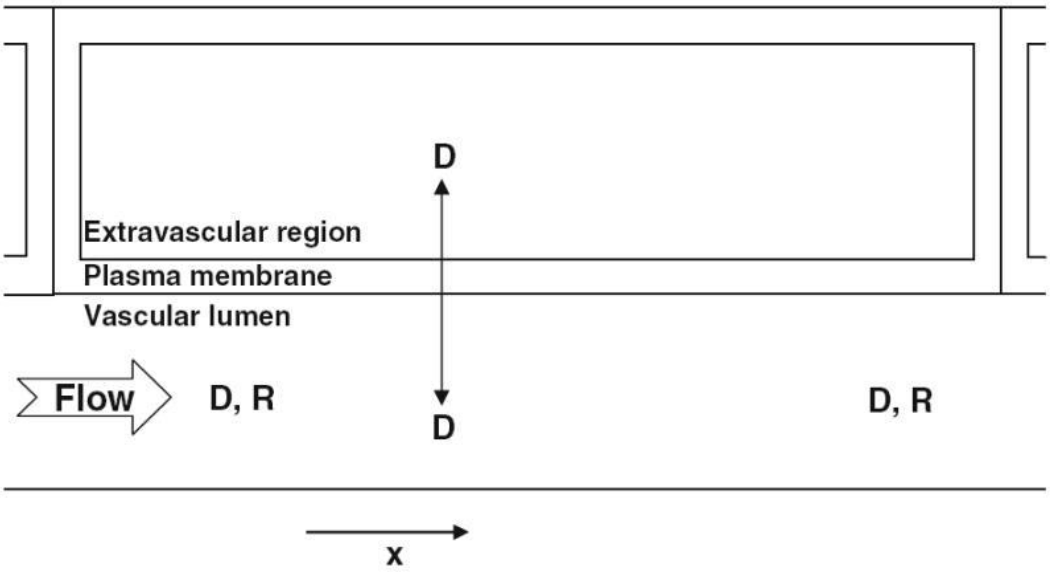

FIGURE 8 A schematic diagram of a single capillary element model for the pulmonary disposition of an intravascular indicator (*R*) and a flow-limited indicator (*D*).

1. The intravascular indicator is confined to the capillary region, whereas the flow-limited test indicator can diffuse out of the capillary region into the extravascular region.

2. Flow is restricted to the vascular region.

3. Transport in the extravascular region is only by diffusion. Diffusion of both intravascular and diffusible indicators in the

direction of flow is negligible as compared with the axial convective transport.

4. With respect to the diffusible indicator, diffusion equilibrium within the vascular and the extravascular volumes in the direction perpendicular to the flow direction is instantaneous.

Under these assumptions, the spatial and temporal variations in the concentrations of the intravascular (R) and flow-limited (D) indicators in the vascular and extravascular regions are described by the following species balance equations:

$$\frac{\partial [R]}{\partial t} + W \frac{\partial [R]}{\partial x} = 0 \tag{A1}$$

$$\frac{\partial [D]}{\partial t} + W \left(\frac{V_c}{V_c + V_e} \right) \frac{\partial [D]}{\partial x} = 0 \tag{A2}$$

where $W = L/t_c$ is the average flow velocity within the capillary region, t_c is the capillary transit time, and $x = 0$ and $x = L$ are the capillary inlet and outlet, respectively. $R(t,x)$ and $D(t,x)$ are the vascular concentration of R and D at distance x from the capillary inlet and time t. The initial conditions are 0 $R(x,0) = D(x,0) = 0$ and the boundary conditions $R(0,t) = D(0,t) = C_{in}(t)$, where $C_{in}(t)$ is the capillary inlet function.

Whole Organ Model To build a capillary bed or an organ, it is assumed that the capillary bed consists of Nx parallel non-interacting capillary elements, each possessing a different transit time t_{ci} (Fig. 9).[6,7] These capillary elements differ only in their length or flow or combination thereof. However, the per-unit capillary vascular volume, exchange surface area, and physical and chemical properties are the same for all capillary elements. Thus, the capillary bed has a distribution of vascular transit times, $h_c(t)$.

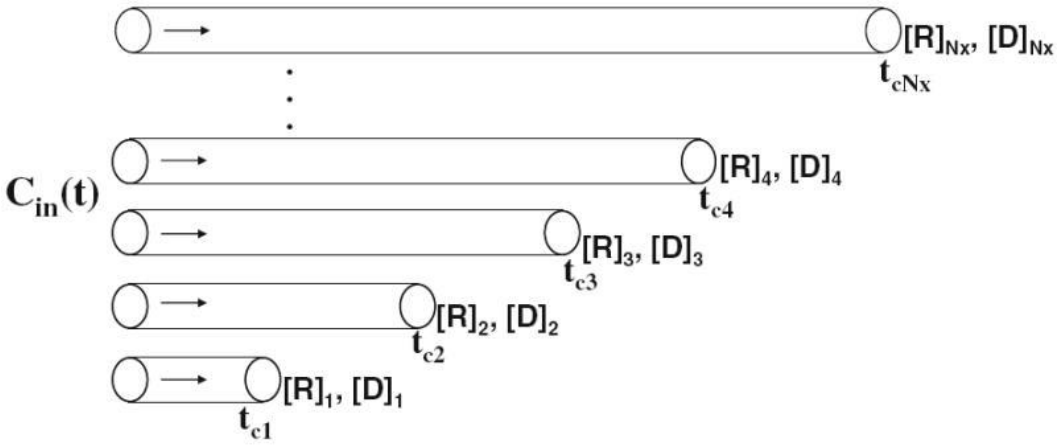

FIGURE 9 Nx parallel pathways corresponding to the *Nx* capillaries with different transit times t_{ci}, i = 1,…, *Nx*. $C_{in}(t)$ is the capillary input function. $[R]_i$ and $[D]_i$ are the concentrations of the intravascular and flow-limited indicators at the outflow of the *i*th capillary element.

The organ model assumes random coupling conditions between the conducting vessels and the exchanging vessels, i.e., all capillary elements are exposed to the same capillary input $C_{in}(t)$. Given the linearity, commutativity, and associativity of the model, $C_{in}(t)$ could be thought of as the outlet concentration curve that would exist if all arteries and veins were connected directly at a common nexus with no intervening capillaries. Thus, $C_{in}(t)$ would include dispersion from the conducting vessels (i.e., arteries and veins), dispersion as a consequence of any tubing connections involved in the sampling or perfusion system, and dispersion resulting from an injection system. Thus, $C_{in}(t) = (q/F)C_{tub}(t)*h_n(t)$ where q is the mass of injected indicator, F is the total flow; $C_{tub}(t)$ is a concentration function representing all dispersive processes occurring outside the organ, including the dispersion caused by the injection system; $h_n(t)$ is the transport function for intravascular and flow-limited diffusible indicators in the conducting vessels of the lung, and * is the convolution operator.

For given values of V_c and $V_e = Ft_e$, and a given $h_c(t)$ and $C_{in}(t)$, each represented by a shifted random walk function (Eq. 3 above) as previously described, the single capillary element equations (Eqs. A1, A2) were solved numerically for each of the *Nx* capillaries with transit times t_i, i = 1,…, *Nx* as shown in Fig. 9.[6,7] Then the capillary outflow concentrations for the intravascular and diffusible indicators $C_R(t)$ and

Annals of Biomedical Engineering, Vol. 38, No. 11 (November 2010): pg. 3449-3465. DOI.

$C_F(t)$ are obtained by summing (doing a mass balance) the outflow concentrations, $[R]_i(t)$ and $[D]_i(t)$, over all Nx capillaries, where each capillary outflow is weighted by its corresponding $H_i = (\Delta t/2)(h_c(t_i - \Delta t/2) + h_c(t_i + \Delta t/2))$, the flow-weighted fraction of capillaries with transit time t_{ci}, and Δt is the transit time increment. Thus,

$$C_{\mathrm{R}}(t) = \sum_{i=1}^{Nx} H_i [R]_i(t) \qquad \text{(A3)}$$

$$C_{\mathrm{D}}(t) = \sum_{i=1}^{Nx} H_i [D]_i(t) \qquad \text{(A4)}$$

Figure 6 shows examples of simulated organ outflow curves of an intravascular indicator and three flow-limited indicators with different extravascular mean residence times ($\bar{t}_e$).

References

1. Albrecht KH, Gaehtgens P, Pries A, Heuser M. The Fahraeus effect in narrow capillaries (i.d. 3.3 to 11.0 micron) Microvasc Res. 1979;18:33–47.

2. Audi SH, Bongard RD, Dawson CA, Siegel D, Roerig DL, Merker MP. Duroquinone reduction during passage through the pulmonary circulation. Am J Physiol Lung Cell Mol Physiol. 2003;285:L1116–L1131.

3. Audi SH, Bongard RD, Krenz GS, Rickaby DA, Haworth ST, Eisenhauer J, Roerig DL, Merker MP. Effect of chronic hyperoxic exposure on duroquinone reduction in adult rat lungs. Am J Physiol Lung Cell Mol Physiol. 2005;289:L788–L797.

4. Audi SH, Bongard RD, Okamoto Y, Merker MP, Roerig DL, Dawson CA. Pulmonary reduction of an intravascular redox polymer. Am J Physiol Lung Cell Mol Physiol. 2001;280:L1290–L1299.

5. Audi SH, Dawson CA, Ahlf SB, Roerig DL. Oxygen dependency of monoamine oxidase activity in the intact lung. Am J Physiol Lung Cell Mol Physiol. 2001;281:L969–L981.

Annals of Biomedical Engineering, Vol. 38, No. 11 (November 2010): pg. 3449-3465. DOI.

6. Audi SH, Krenz GS, Linehan JH, Rickaby DA, Dawson CA. Pulmonary capillary transport function from flow-limited indicators. J Appl Physiol. 1994;77:332–351.

7. Audi SH, Linehan JH, Krenz GS, Dawson CA. Accounting for the heterogeneity of capillary transit times in modeling multiple indicator dilution data. Ann Biomed Eng. 1998;26:914–930.

8. Audi SH, Linehan JH, Krenz GS, Dawson CA, Ahlf SB, Roerig DL. Estimation of the pulmonary capillary transport function in isolated rabbit lungs. J Appl Physiol. 1995;78:1004–1014.

9. Audi SH, Merker MP, Krenz GS, Ahuja T, Roerig DL, Bongard RD. Coenzyme Q1 redox metabolism during passage through the rat pulmonary circulation and the effect of hyperoxia. J Appl Physiol. 2008;105:1114–1126.

10. Audi SH, Olson LE, Bongard RD, Roerig DL, Schulte ML, Dawson CA. Toluidine blue O and methylene blue as endothelial redox probes in the intact lung. Am J Physiol Heart Circ Physiol. 2000;278:H137–H150.

11. Audi SH, Zhao H, Bongard RD, Hogg N, Kettenhofen NJ, Kalyanaraman B, Dawson CA, Merker MP. Pulmonary arterial endothelial cells affect the redox status of coenzyme Q0. Free Radic Biol Med. 2003;34:892–907.

12. Bassingthwaighte JB, Ackerman FH, Wood EH. Applications of the lagged normal density curve as a model for arterial dilution curves. Circ Res. 1966;18:398–415.

13. Bassingthwaighte JB, Goresky CA, Linehan JH. Whole Organ Approaches to Cellular Metabolism: Permeation, Cellular Uptake, and Product Formation. New York: Springer; 1998.

14. Beasley R, Aldington S, Weatherall M, Robinson G, McHaffie D. Oxygen therapy in myocardial infarction: an historical perspective. J R Soc Med. 2007;100:130–133.

15. Bhandari V, Choo-Wing R, Lee CG, Zhu Z, Nedrelow JH, Chupp GL, Zhang X, Matthay MA, Ware LB, Homer RJ, Lee PJ, Geick A, de Fougerolles AR, Elias JA. Hyperoxia causes angiopoietin 2-mediated acute lung injury and necrotic cell death. Nat Med. 2006;12:1286–1293.

16. Bongard RD, Krenz GS, Linehan JH, Roerig DL, Merker MP, Widell JL, Dawson CA. Reduction and accumulation of methylene blue by the lung. J Appl Physiol. 1994;77:1480–1491.

17. Bongard RD, Merker MP, Shundo R, Okamoto Y, Roerig DL, Linehan JH, Dawson CA. Reduction of thiazine dyes by bovine pulmonary arterial endothelial cells in culture. Am J Physiol. 1995;269:L78–L84.

18. Cadenas E, Boveris A, Ragan CI, Stoppani AO. Production of superoxide radicals and hydrogen peroxide by NADH-ubiquinone reductase and ubiquinolcytochrome *c* reductase from beef-heart mitochondria. Arch Biochem Biophys. 1977;180:248–257.

19. Capellier G, Maupoil V, Boussat S, Laurent E, Neidhardt A. Oxygen toxicity and tolerance. Minerva Anestesiol. 1999;65:388–392.

20. Clough AV, Haworth ST, Hanger CC, Wang J, Roerig DL, Linehan JH, Dawson CA. Transit time dispersion in the pulmonary arterial tree. J Appl Physiol. 1998;85:565–574.

21. Crapo JD, Barry BE, Foscue HA, Shelburne J. Structural and biochemical changes in rat lungs occurring during exposures to lethal and adaptive doses of oxygen. Am Rev Respir Dis. 1980;122:123–143.

22. Crapo JD, Peters-Golden M, Marsh-Salin J, Shelburne JS. Pathologic changes in the lungs of oxygen-adapted rats: a morphometric analysis. Lab Invest. 1978;39:640–653.

23. Crapo JD, Tierney DF. Superoxide dismutase and pulmonary oxygen toxicity. Am J Physiol. 1974;226:1401–1407.

24. Dawson CA, Audi SH, Bongard RD, Okamoto Y, Olson L, Merker MP. Transport and reaction at endothelial plasmalemma: distinguishing intra- from extracellular events. Ann Biomed Eng. 2000;28:1010–1018.

25. Dawson CA, Audi SH, Krenz GS, Roerig DL. Endothelium and compound transfer. In: Feinendegen LE, Shreeve WW, Eckelman WC, Bahk YW, Wagner HN Jr, editors. Molecular Nuclear Medicine: The Challenge of Genomics and Proteomics to Clinical Practice. New York: Springer; 2003. pp. 201–216.

26. Fisher AB. Oxygen utilization and toxicity in the lungs. In: Fishman AP, editor. Handbook of Physiology: The Respiratory System. Bethesda: Williams & Wilkins; 1987. pp. 231–254.

27. Fisher AB, Beers MF. Hyperoxia and acute lung injury. Am J Physiol Lung Cell Mol Physiol. 2008;295:L1066.

28. Frank L, Iqbal J, Hass M, Massaro D. New "rest period" protocol for inducing tolerance to high O_2 exposure in adult rats. Am J Physiol. 1989;257:L226–L231.

29. Freeman BA, Crapo JD. Biology of disease: free radicals and tissue injury. Lab Invest. 1982;47:412–426.

30. Freeman BA, Topolosky MK, Crapo JD. Hyperoxia increases oxygen radical production in rat lung homogenates. Arch Biochem Biophys. 1982;216:477–484.

31. Gonzalez-Fernandez JM, Atta SE. Maximal substrate transport in capillary networks. Microvasc Res. 1973;5:180–198.

32. Goresky CA. A linear method for determining liver sinusoidal and extravascular volumes. Am J Physiol. 1963;204:626–640.

33. Guntheroth WG, Luchtel DL, Kawabori I. Pulmonary microcirculation: tubules rather than sheet and post. J Appl Physiol. 1982;53:510–515.

34. Heffner JE, Repine JE. Pulmonary strategies of antioxidant defense. Am Rev Respir Dis. 1989;140:531–554.

35. Ho YS, Dey MS, Crapo JD. Antioxidant enzyme expression in rat lungs during hyperoxia. Am J Physiol. 1996;270:L810–L818. [

36. Howell K, Preston RJ, McLoughlin P. Chronic hypoxia causes angiogenesis in addition to remodelling in the adult rat pulmonary circulation. J Physiol. 2003;547:133–145.

37. Jamieson D, Chance B, Cadenas E, Boveris A. The relation of free radical production to hyperoxia. Annu Rev Physiol. 1986;48:703–719.

38. Kim V, Benditt JO, Wise RA, Sharafkhaneh A. Oxygen therapy in chronic obstructive pulmonary disease. Proc Am Thorac Soc. 2008;5:513–518.

39. Kimball RE, Reddy K, Peirce TH, Schwartz LW, Mustafa MG, Cross CE. Oxygen toxicity: augmentation of antioxidant defense mechanisms in rat lung. Am J Physiol. 1976;230:1425–1431.

40. Kwak DJ, Kwak SD, Gauda EB. The effect of hyperoxia on reactive oxygen species (ROS) in rat petrosal ganglion neurons during development using organotypic slices. Pediatr Res. 2006;60:371–376.

41. Lenaz G. Quinone specificity of complex I. Biochim Biophys Acta. 1998;1364:207–221.

42. Mercer RR, Crapo JD. Three-dimensional reconstruction of the rat acinus. J Appl Physiol. 1987;63:785–794.

43. Merker MP, Audi SH, Bongard RD, Lindemer BJ, Krenz GS. Influence of pulmonary arterial endothelial cells on quinone redox status: effect of hyperoxia-induced NAD(P)H:quinone oxidoreductase 1. Am J Physiol Lung Cell Mol Physiol. 2006;290:L607–L619.

44. Merker MP, Bongard RD, Kettenhofen NJ, Okamoto Y, Dawson CA. Intracellular redox status affects transplasma membrane electron transport in pulmonary arterial endothelial cells. Am J Physiol Lung Cell Mol Physiol. 2002;282:L36–L43.

45. Miller WS. The Lung. Springfield, IL: Charles C. Thomas; 1947.

46. Presson RG, Jr, Graham JA, Hanger CC, Godbey PS, Gebb SA, Sidner RA, Glenny RW, Wagner WW., Jr Distribution of pulmonary capillary red blood cell transit times. J Appl Physiol. 1995;79:382–388.

47. Presson RG, Jr, Todoran TM, De Witt BJ, McMurtry IF, Wagner WW., Jr Capillary recruitment and transit time in the rat lung. J Appl Physiol. 1997;83:543–549.

48. Randell SH, Mercer RR, Young SL. Neonatal hyperoxia alters the pulmonary alveolar and capillary structure of 40-day-old rats. Am J Pathol. 1990;136:1259–1266.

49. Saugstad OD. Optimal oxygenation at birth and in the neonatal period. Neonatology. 2007;91:319–322.

50. Schwab AJ, Goresky CA. Hepatic uptake of protein-bound ligands: effect of an unstirred Disse space. Am J Physiol. 1996;270:G869–G880.

51. Shi W, Eidelman DH, Michel RP. Differential relaxant responses of pulmonary arteries and veins in lung explants of guinea pigs. J Appl Physiol. 1997;83:1476–1481.

52. Sjostrom K, Crapo JD. Structural and biochemical adaptive changes in rat lungs after exposure to hypoxia. Lab Invest. 1983;48:68–79.

53. Staub NC, Schultz EL. Pulmonary capillary length in dogs, cat and rabbit. Respir Physiol. 1968;5:371–378.

54. Turrens JF, Freeman BA, Levitt JG, Crapo JD. The effect of hyperoxia on superoxide production by lung submitochondrial particles. Arch Biochem Biophys. 1982;217:401–410.

55. Valenca Sdos S, Kloss ML, Bezerra FS, Lanzetti M, Silva FL, Porto LC. Effects of hyperoxia on Wistar rat lungs. J Bras Pneumol. 2007;33:655–662.

56. West JB, Wagner PD. Ventilation-perfusion relationships. In: Crystal RG, West JB, Weibel ER, Barnes PJ, editors. The Lung: Scientific Foundations. Philadelphia: Lippincott-Raven; 1997. pp. 1693–1709.

57. Zierhut ML, Gardner JC, Spilker ME, Sharp JT, Vicini P. Kinetic modeling of contrast-enhanced MRI: an automated technique for assessing inflammation in the rheumatoid arthritis wrist. Ann Biomed Eng. 2007;35:781–795.

About the Authors

Said H. Audi: said.audi@marquette.edu